



Natural Ventilation

Xiaohong Zheng, Zhenni Shi, Zheqi Xuan, and Hua Qian

Contents

Introduction	1228
Prediction of Natural Ventilation	1230
Single-Zone Model	1231
Multi-Zone Model	1237
Computational Fluid Dynamics (CFD) Model	1242
The Influence of Porous Screens on Ventilation Rate	1244
Measurement of Natural Ventilation Rate	1246
Tracer Gas Method	1246
Air Velocity Measuring Method	1250
Natural Ventilation Form	1250
General Natural Ventilation Form	1250
Methods to Enhance the Natural Ventilation Performance	1252
Design for Natural Ventilation	1256
General Procedure for Natural Ventilation Design	1256
Vent Sizing	1257
Natural Ventilation in Industrial Buildings	1260
Example for Natural Ventilation	1264
Conclusion and Future Directions	1267
References	1269

Abstract

Proper utilization of natural ventilation can provide large ventilation rate without the consumption of energy. This chapter introduces the prediction, measurement, form, and design of natural ventilation along with an example. The prediction model includes single-zone model, multi-zone model, and CFD model, among which CFD model is the most frequently used tool to analyze airflow distribution

X. Zheng (✉) · Z. Shi · Z. Xuan · H. Qian
School of Energy and Environment, Southeast University, Nanjing, China
e-mail: xhzheng@seu.edu.cn; qianh@seu.edu.cn; Keenwa@gmail.com

inside or around buildings. Porous screens fixed on openings to prevent insects and particulates could increase the airflow resistance through openings, resulting in great reduction in ventilation rate. Tracer gas methods are considered as the most commonly utilized method to measure ventilation rate, especially the tracer gas concentration decay method. As natural ventilation is driven by wind or buoyancy, the commonly used natural ventilated building form includes wind-driven ventilation form, buoyancy-driven ventilation form, and the combination of those two. In addition, measures which can be used to enhance natural ventilation performance such as atrium ventilation, ventilation cap, and solar chimney are also involved. A general procedure of natural ventilation design includes architectural plan, system layout, component selection, vent sizing, control strategy development, and detailed design drawing. The opening size is calculated based on factors such as certain geometry, climate, and building's configuration. The methods of opening size calculation consist of direct methods and indirect methods. Direct methods are derived from simple buildings where the ventilation rate is a simple function of the governing parameters. Indirect methods try different opening size combinations and identify the best one based on network models. Besides, an existing architecture example and its natural ventilation performance are also introduced.

Keywords

Natural ventilation · Ventilation rate · Multi-zone model · Porous screens · Cross-ventilation

Introduction

With the development of economic and the improvement of people's living standard, people spend more and more time staying inside buildings. According to Wang [1], most people spend 70%–90% of their time indoors. Volatile organic compounds (VOC) released from buildings, furnishings, cooking, smoking, and inorganic compounds generated from people's metabolism (especially CO₂) are indoor air pollutants which cannot be neglected [2]. Ventilation is the most direct and effective way to dilute indoor air pollutants as well as satisfy occupants' thermal and wet comfort.

Natural ventilation is the flow of outdoor air caused by wind and thermal pressures through intentional openings in the building's shell [3]. The application of natural ventilation possesses a long history. Evidence of the use of natural ventilation in China can date back to the Neolithic period. Natural ventilation technology varies with regions as the local climate conditions change. For example, people in Xishuangbanna use bamboo ventilation buildings to acclimatize themselves to hot and humid climate, while people in Xinjiang base on thick walls to accommodate dry and hot climate. As a Chinese philosophical system of harmonizing people with the surrounding environment, *feng shui* was extensively used to orient buildings depending on wind, water, mountains, and so on [4]. *Feng shui* advocates utilizing wind gently. Besides, rational space and orientation are also

involved in *feng shui* theory. At the end of the twentieth century, China has gradually carried out research on traditional suitable technology in the field of construction technology. However, the fact that natural ventilation depends too much on the climate conditions makes it difficult to guarantee adequate control of thermal comfort and indoor air quality (IAQ) all the time [3]. It is in the past 150 years or so that mechanical ventilation has been widely used in public buildings such as hospitals and commercial buildings where good IAQ needs to be ensured.

The energy crisis in the 1970s evoked an urgent need to reduce energy consumption [5]. Building energy consumption accounts for about 20%–25% of the total delivered energy consumed worldwide, which has been increased by an average of 1.5% per year from 2012 to 2040 for OECD nations [6, 7]. The average energy consumption of a mechanical HVAC system occupies 50%–60% of total building energy consumption [8, 9]. To save energy, ASHRAE Standard 119 [10] and the National Building Code of Canada [11] encourage to strengthen the tightness of buildings which could result in poor natural ventilation performance. Inadequate ventilation performance would finally cause sick building syndrome (SBS) and building-related illness (BRI) for occupants in the buildings. Due to the expected threat of influenza pandemic, the ventilation rate and air distribution in hospitals have received increasing attention, especially after the epidemics of the severe acute respiratory syndrome (SARS) in 2003 [12]. In order to minimize the cross infection risk in hospitals and isolation rooms, engineering control methods were suggested in airborne infection isolation (AII) rooms [13]. The ventilation rate is stipulated to 12ACH at least, and the airflow is strictly ruled to flow from clean area to dirty area [13]. Although higher ventilation rate is able to provide a higher dilution capability, it also indicates a higher energy cost and equipment cost for a ventilation system. In terms of some developing countries like Slovenia, such high-cost AII rooms are difficult to construct [14]. Even among the constructed AII rooms, many of them cannot meet the CDC standard [15–18]. Assuming the indoor air is well-mixed, the infection risk of airborne transmission diseases can be calculated from the classical Wells-Riley equation [19], as shown in Eq. (1):

$$P = \frac{Case}{S} = 1 - e^{-I_{qr}t/Vn} \quad (1)$$

where P is the risk of airborne-transmitted diseases, p is the pulmonary ventilation rate of each susceptible per minute (m^3/h), n is the air change rate (ACH), q is the quanta produced by one infector (quanta/h), a quantum of infection is the dose which is necessary to lead infection to a new susceptible and may be one or more airborne particles, V is the volume of enclosed space (m^3), and t is the duration of exposure (h). The higher the ventilation rate, the lower the risk of airborne-transmitted diseases. According to Qian's field measurement [12], natural ventilation can provide up to 69 ACH high ventilation rate when all the openings are open. With appropriate installation of mechanical exhaust fans, a reasonable negative pressure can be created which makes it possible to convert an existing naturally ventilated ward into a temporary isolation room. Actually, the use of natural ventilation to treat

tuberculosis could be traced back to more than 100 years ago [20]. As natural ventilation has great potential to remove indoor air pollutants, an increasingly number of studies are carried out to apply natural ventilation in hospitals for infection control [12, 21–25].

In general, natural ventilation can provide a high ventilation rate more economically than mechanical ventilation, yet its airflow and temperature are difficult to predict and control. The mass and energy conservation models of multi-zone natural ventilation buildings are highly nonlinear equations that make the prediction of natural ventilation complex. It is challenging to analyze the qualitative and quantitative solutions of such nonlinear dynamic systems. The results are diversiform and vary with initial conditions. Even with exact initial conditions, the solution may be divergent due to very small disturbances. However, the modern natural ventilation is also technology-dependent, which is the same as mechanical systems. Different from traditional natural ventilation systems, natural ventilation today depends on modern computer control system, modern design of ventilation openings, assisting fan design, etc. Therefore, if properly designed, natural ventilation can also be reliable, especially when combined with a mechanical system using the hybrid ventilation principle [26].

This chapter will introduce a general introduction to natural ventilation. At first, it provides the reasonably comprehensive prediction and measurement of natural ventilation. Secondly, it summarizes the natural ventilation form and methods to enhance the performance. The third part aims to describe how to design a natural ventilation building and provide some examples.

Prediction of Natural Ventilation

Natural ventilation supplies air and removes air from an indoor space without using mechanical systems. It can provide high ventilation rate with little energy consumption. Almost no equipment is needed to occupy areas. Besides, the initial and operating costs are also lower than those of mechanical ventilation. However, natural ventilation rate and air distribution are greatly dependent on outdoor climate, making them difficult to analyze and predict.

There are various analytical methods for natural ventilation. Firstly, the single-zone model based on the analysis of pressure difference is easy to understand and apply, but it is limited to simple buildings only. Secondly, the multi-zone models such as COMIS and MIX can be used to calculate large buildings with high computation speed, yet it is complicated to operate, and the results are not intuitive to display. Thirdly, some CFD software such as Fluent, FloVENT, STAR-CD, and Phoenix can describe the airflow distribution inside and around the building with very intuitive results, but the operation is complicated and the computation is time-consuming. Finally, experiments such as salt-bath scaled model or full-scale experiment can deflect some physical characteristics of natural ventilation, and the results are reliable, but these cost a lot of labor and resources to operate.

Single-Zone Model

There are two types of natural ventilation occurring in buildings, respectively, wind-driven ventilation and buoyancy-driven ventilation. Wind-driven ventilation arises from different pressures created by wind around and flows into a building through openings on external envelopes. Buoyancy-driven ventilation occurs due to the directional buoyancy force generated by temperature differences between the interior and exterior [27]. The air will flow through the window if the pressure difference (ΔP) driven by wind or temperature difference exists on both sides of the window. Besides, the resistance of air flowing through the window is equal to ΔP :

$$\Delta P = \zeta \frac{\rho v^2}{2} \tag{2}$$

where ΔP (Pa) is pressure difference between the two sides of the calculated window, v (m/s) is the velocity of air flowing through the window, ρ (kg/m³) is air density, and ζ is the local resistance coefficient of the window.

Equation (2) can be changed into

$$v = \sqrt{\frac{2\Delta P}{\zeta\rho}} = C_d \sqrt{\frac{2\Delta P}{\rho}} \tag{3}$$

where C_d is the discharge coefficient of the window related to the construction of the window $C_d = \sqrt{1/\xi}$. In general, C_d is equal to 0.61.

The rate of air flowing through the window can be calculated as

$$q_v = \nu A = C_d A \sqrt{\frac{2\Delta P}{\rho}} \tag{4}$$

$$q = \rho \cdot L = C_d A \sqrt{2\rho\Delta P} \tag{5}$$

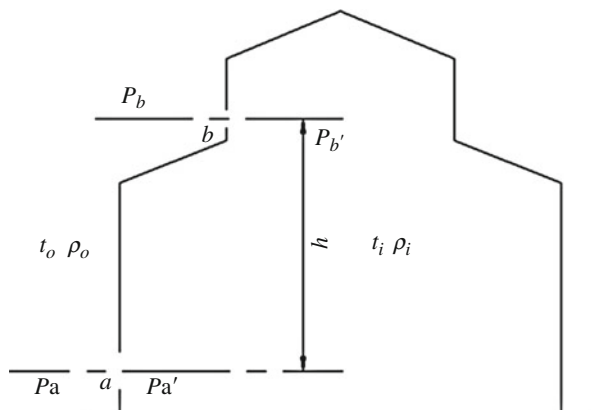
where A (m²) is the area of the window, q_v (m³/s) is the volume ventilation rate, and q (kg/s) is the mass ventilation rate.

According to the above equations, if the pressure difference ΔP between the two sides of the calculated window and the window area A remains known, the ventilation rate q through the window can be obtained.

Natural Ventilation Driven by Buoyancy

As illustrated in Fig. 1, a building has two equal-area windows (a and b) at different heights on the same side of the external envelope. The letter h represents the height difference between the two windows; P_a and P_b represent the static pressure at the same height of the windows a and b , respectively, outside the building; and P'_a and P'_b represent the static pressure at the same height of the windows a and b , respectively, inside the building. t_i and t_o stand for the indoor and outdoor air

Fig. 1 Buoyancy-driven ventilation



temperatures, respectively. ρ_i and ρ_o indicate the indoor and outdoor air densities, respectively. If $t_i > t_o$, $\rho_i < \rho_o$.

According to the theory of fluid statics, the internal-external pressure difference (ΔP_b) at window b can be expressed as

$$\begin{aligned} \Delta P_b &= (P_b' - P_b) = (P_a' - gh\rho_i) - (P_a - gh\rho_o) \\ &= (P_a' - P_a) + gh(\rho_o - \rho_i) \\ &= \Delta P_a + gh(\rho_o - \rho_i) \end{aligned} \quad (6)$$

where ΔP_a (Pa) and ΔP_b (Pa) are internal and external pressure differences at windows a and b ; if $\Delta P > 0$, the air flows out. If $\Delta P < 0$, the air flows in; g (m/s²) is gravity acceleration.

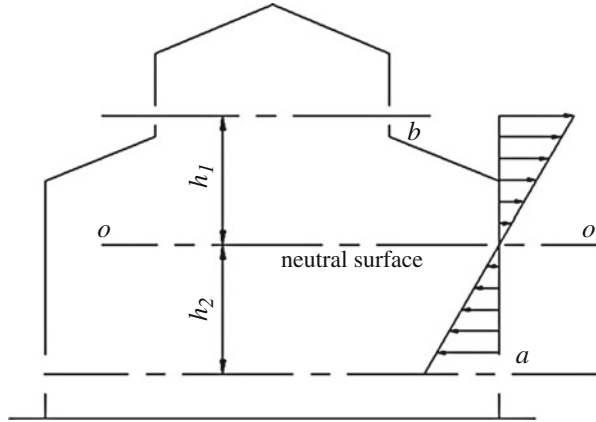
According to Eq. (6), if $\Delta P_a = 0$, as long as $\rho_o > \rho_i$ ($t_i > t_o$), $\Delta P_b > 0$. Therefore, when both windows a and b are open, air will flow out through window b . With the indoor air flowing out, static pressure inside gradually decreases. The value ($P_a' - P_a$) varies from 0 to minus; at the same time, the outdoor air flows in through window a . When the air supply rate of window a equals to the air exhaust rate of window b , the indoor static pressure becomes stable. When air flows in through window a , $\Delta P_a < 0$; when air flows in from window b , $\Delta P_b < 0$.

Equation (6) can be changed into

$$\Delta P_b + (-\Delta P_a) = \Delta P_b + |\Delta P_a| = gh(\rho_o - \rho_i) \quad (7)$$

Equation (7) shows that the sum of the absolute pressure differences at the supply and exhaust windows is related to the height difference h between the two windows and the air density difference ($\rho_o - \rho_i$) inside and outside the building. The term $gh(\rho_o - \rho_i)$ is defined as the buoyancy pressure. If there exists no air temperature difference between the indoor and outdoor windows or no height difference between the windows, natural ventilation will not occur. Actually, natural ventilation can also

Fig. 2 Variation of the pressure difference along the height of the building



occur with only one window. The upper part of the window exhausts air, and the lower part supplies air under such circumstances. It is equivalent to the condition that the two windows become together.

Without special explanation, “pressure difference” represents the static pressure difference between a certain point inside the building and another point of the same height outside the building, taken as P_x . The pressure difference at window a is indicated as P_{xa} . If P_{xa} is bigger than 0, the air flows out. If P_{xa} is less than 0, the air flows in. If the center plane of window a is taken as the datum, the pressure difference at the calculated window can be obtained as

$$P'_x = P_{xa} + gh'(\rho_o - \rho_i) \tag{8}$$

where P'_x (Pa) is internal pressure difference at the calculated window, P_{xa} (Pa) is internal pressure difference at window a , and h' is the height difference between the calculated window and window a . The greater the height difference h' , the greater the pressure difference at the calculated window. As static pressure of each point in the same horizontal plane is equal, the pressure difference at a window is equal to that at each point on the center plane of the calculated window. Under the buoyancy pressure effect, the pressure difference along the height of the building changes is shown in Fig. 2. The values of the pressure difference increase gradually from negative at the air supply window to positive at the exhaust window. The surface where the pressure difference equals zero is defined as neutral surface, and Fig. 2 shows surface $o-o$. No air flows through the neutral surface.

If the neutral surface is taken as the datum plane, the pressure difference at window a is

$$P_{xa} = P_{xo} - h_1(\rho_o - \rho_i)g = -h_1(\rho_o - \rho_i)g \tag{9}$$

The pressure difference at window b is

$$P_{xb} = P_{xo} + h_2(\rho_o - \rho_i)g = h_2(\rho_o - \rho_i)g \quad (10)$$

where P_{xo} is pressure difference on the neutral surface, which is equal to zero; h_1 is the height between window a and the neutral surface; and h_2 is the height between window b and the neutral surface.

Equations (9) and (10) present that the absolute value of the pressure difference at a certain window is related to the height between the neutral surface and the calculated window. If $t_i > t_o$, the pressure difference above the neutral surface is positive, causing air flowing out of the window. The pressure difference below the neutral surface is negative, which leads to air flowing in the window.

Natural Ventilation Driven by Wind

When wind flows around a building, the pressure distribution of wind will change due to the obstruction of the building. On the windward side, the static pressure increases when the kinetic pressure decreases. On the side surface and leeward surface, the static pressure decreases due to the local vortex. The increase or decrease of the static pressure causes wind pressure on the building surface. When the static pressure increases, the wind pressure is positive. Otherwise, the wind pressure is negative.

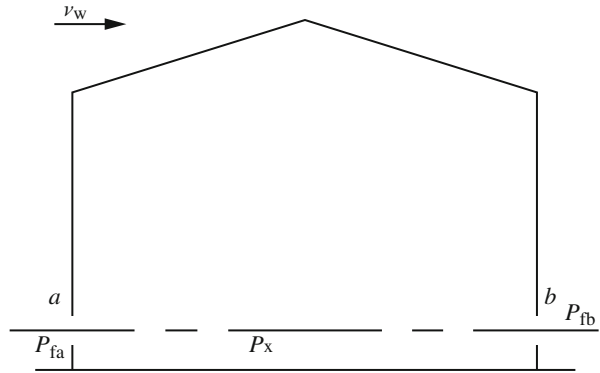
The wind pressure distribution around a building is related to the geometry of the building and the outdoor wind direction. When the wind direction is constant, the wind-driven pressure at a certain point on the external building envelope can be expressed as follows:

$$P_f = C_P \frac{v_o^2}{2} \rho_o \quad (11)$$

where C_P is wind pressure coefficient, v_o (m/s) is outdoor air velocity, and ρ_o (kg/m³) is outdoor air density.

On the external envelope of a building, if there are two windows with different wind pressures, the window with larger wind pressure coefficient will supply air, and the other one will exhaust air. If the temperature difference between the inside and outside is zero, no buoyancy pressure occurs. As presented in Fig. 3, the wind speed is represented as v_w , the wind pressure on the windward window is P_{fa} , and the wind-driven pressure on the leeward window is P_{fb} ($P_{fa} > P_{fb}$). The pressure difference on the central plane of the window is P_x . Without the effect of buoyancy pressure, the pressure difference at each point inside the room keeps equal. If window a is open and window b is closed, the indoor pressure difference gradually increases due to the effect of wind-driven pressure. When the indoor pressure difference is equal to the wind-driven pressure ($P_x = P_{fa}$), the air stops flowing. If both window a and window b are open, the air will flow out through window b as $P_{fa} > P_{fb}$ and $P_x = P_{fa}$, $P_x > P_{fb}$. With the air flowing out, the pressure difference P_x decreases until $P_{fa} > P_x$. The outdoor air flows into the room through window a when $P_{fa} > P_x$. It keeps stable ($P_{fa} > P_x > P_{fb}$) when the air supply rate through window a is equal to the air exhaust rate through window b .

Fig. 3 Wind-driven ventilation



The distribution of wind pressure coefficient C_p on buildings' surfaces varies with the geometries of buildings and the wind direction. C_p on the windward side is positive, while that on the roof side and the leeward side remains negative. Whether C_p on the side face is positive or negative depends on the angle relative to the main wind direction. Figure 4a, b illustrates the distribution of wind pressure coefficient on building' surfaces with flat roof and with slope roof, respectively. The airflow rate through an opening depends on the pressure both outside and inside. The inside pressure can be calculated through law of mass conservation if wind pressure is the only source of the inside pressure and no separator exists inside the building. Considering there is a building with four walls numbered from 1 to 4, each wall has an equal-area opening. If the outside wind pressure coefficient is C_{pn} ($n = 1..4$), the inside wind pressure coefficient is C_{pi} , and the airflow rates in or out the openings are proportional to the square root of the difference between the inside and outside wind pressures, as shown in Eq. (12):

$$q_n \propto \sqrt{C_{pn} - C_{pi}} \tag{12}$$

If airflow is supplied through opening 1 ($C_{p1} > 0$) and removed through opening 2-4 ($C_{p2,3,4} < 0$), the inside wind pressure coefficient can be calculated by Eq. (13):

$$|(C_{p1} - C_{pi})|^{1/2} = \sum_{n=2}^4 |(C_{pi} - C_{pn})|^{1/2} \tag{13}$$

If there are separators inside the building and both outer wall and interior wall have equal-area openings, the inside wind pressure coefficient of each cubicle can be calculated through using the above method separately. If the openings' areas are not equal, the openings' areas should be counted in, which can be found in Eqs. (14), (15), and (16) [28]:

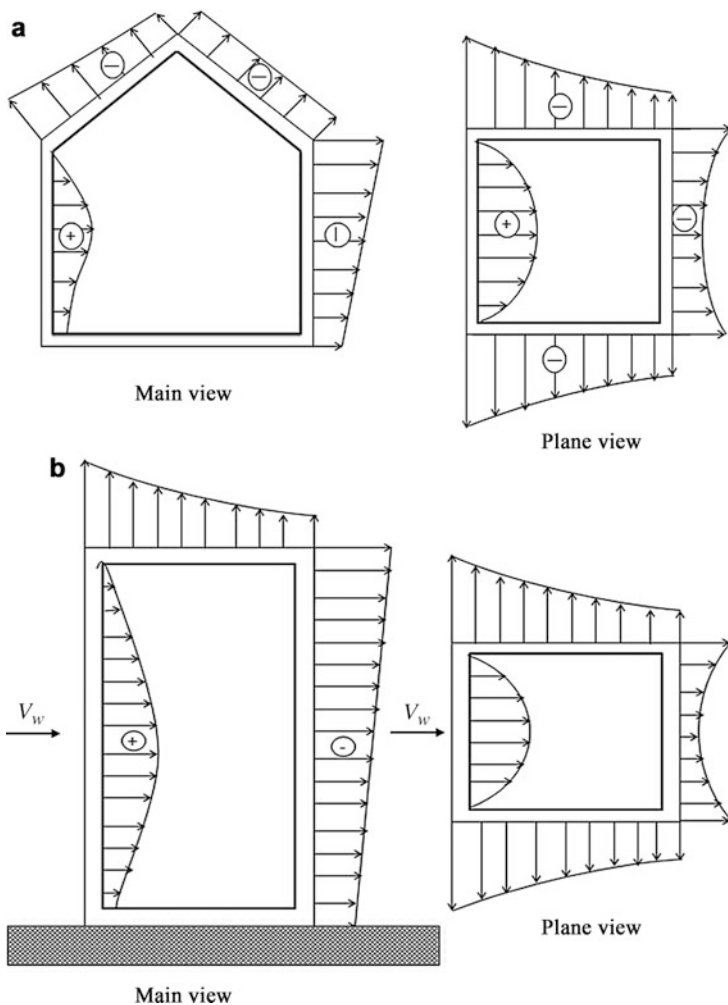


Fig. 4 The distribution of wind pressure coefficient on buildings' surfaces. (a) Building with flat roof. (b) Building with slope roof

$$q = (C_d A)^* \sqrt{2\Delta P / \rho_0} \tag{14}$$

$$(C_d A)^* = \sqrt{\frac{1}{(C_{d1} A_1)^2} + \frac{1}{(C_{d2} A_2)^2}} \tag{15}$$

$$\Delta P = \frac{1}{2} \rho_0 \bar{v}^2 |(C_{pn} - C_{pi})| \tag{16}$$

Liddament [29] analyzed the C_p values on different surfaces of a three-story-high square building and a rectangle building under the consideration of the building

group around and wind direction. The results can be used to calculate ventilation rate roughly according to Tables 1 and 2.

Natural Ventilation Driven by Wind and Buoyancy

When a building (as shown in Fig. 7) is affected by both wind pressure and buoyancy pressure, the total pressure difference between the inside and outside of the calculated window is equal to the sum of the wind-driven pressure difference and buoyancy pressure difference. Besides, it is equal to the outdoor wind pressure subtracting the static pressure difference between the inside and outside at the same height. The total pressure difference at window a can be expressed as

$$\Delta P_a = P_{xa} - C_{p,a} \frac{v_o^2}{2} \rho_o \quad (17)$$

The total pressure difference at window b is

$$\Delta P_b = P_{xb} - C_{p,b} \frac{v_o^2}{2} \rho_o = P_{xa} + hg(\rho_o - \rho_i) - C_{p,b} \frac{v_o^2}{2} \rho_o \quad (18)$$

where P_{xa} (Pa) is the pressure difference at window a ; P_{xb} (Pa) is the pressure difference at window b ; $C_{p,a}$ and $C_{p,b}$ are the wind pressure coefficient of window a and b , respectively; and h indicates the height difference between windows a and b .

The wind speed and direction change frequently and are not stable at all. Therefore, the effect of buoyancy pressure in the actual calculation rather than wind-driven pressure should be taken into consideration to ensure the design effect of natural ventilation. However, the influence of wind-driven pressure on natural ventilation must be qualitatively considered.

Multi-Zone Model

The multi-zone model is derived from the single-zone model which assumes the entire building as a control volume. In the single-zone model, the interior of the building is considered to be a single, well-mixed region, and the pressure and temperature distributions are uniform, suggesting only one node exists in pressure difference calculation. The internal pressure point is connected to an external pressure point or to a plurality of external nodes with different pressures. Compared with the multi-zone model, although the single-zone model requires fewer conditions, it cannot provide the airflow distribution of the external wall.

Multi-zone model assumes that the distribution of the characteristic parameters of each room are uniform which means a room in the building is regarded as a node and it can be connected to other rooms through windows, doors, crevices, etc. Multi-zone model uses the Bernoulli equation to solve the pressure on both sides of the opening and then calculates the airflow based on the relationship between pressure and flow. It is only suitable for predicting the ventilation rate of the multi-zone buildings whose

Table 1 The C_p values on difference surfaces of a building like Fig. 5 [29]

Surface	C_p values, wind direction α							
	0	45	90	135	180	225	270	315
(a) Without block (the building is located in an open area)								
1	0.7	0.35	-0.5	-0.4	-0.2	-0.4	-0.5	-0.35
2	-0.2	-0.4	-0.5	0.35	0.7	0.35	-0.5	-0.4
3	-0.5	0.35	0.7	0.35	-0.5	-0.4	-0.2	-0.4
4	-0.5	-0.4	-0.2	-0.4	-0.5	0.35	0.7	0.35
The angle of the roof is $<10^\circ$								
Front	-0.8	-0.7	-0.6	-0.5	-0.4	-0.5	-0.6	-0.7
Back	-0.4	-0.5	-0.6	-0.7	-0.8	-0.7	-0.6	-0.5
The angle of the roof is $11^\circ-30^\circ$								
Front	-0.4	-0.5	-0.6	-0.5	-0.4	-0.5	-0.6	-0.7
Back	-0.4	-0.5	-0.6	-0.5	-0.4	-0.5	-0.6	-0.5
The angle of the roof is $>30^\circ$								
Front	0.3	-0.4	-0.6	-0.4	-0.5	-0.4	-0.6	-0.4
Back	-0.5	-0.4	-0.6	-0.4	-0.3	-0.4	-0.6	-0.4
(b) With some block (the building is located in an open area with some lower constructions around)								
1	0.4	0.1	-0.3	-0.35	-0.2	-0.35	-0.3	-0.1
2	-0.2	-0.35	-0.3	0.1	0.4	0.1	-0.3	-0.35
3	-0.3	0.1	0.4	0.1	-0.3	-0.35	-0.2	-0.35
4	-0.3	-0.35	-0.2	-0.35	-0.3	0.1	0.4	0.1
The angle of the roof is $<10^\circ$								
Front	-0.6	-0.5	-0.4	-0.5	-0.6	-0.5	-0.4	-0.5
Back	-0.6	-0.5	-0.4	-0.5	-0.6	-0.5	-0.4	-0.5
The angle of the roof is $11^\circ-30^\circ$								
Front	-0.35	-0.45	-0.55	-0.45	-0.35	-0.45	-0.55	-0.45
Back	-0.35	-0.45	-0.55	-0.45	-0.35	-0.45	-0.55	-0.45
The angle of the roof is $>30^\circ$								
Front	0.3	-0.5	-0.6	-0.5	-0.5	-0.5	-0.6	-0.5
Back	-0.5	-0.5	-0.6	-0.5	-0.3	-0.5	-0.6	-0.5
(c) With block (the building is located in downtown area with high constructions around)								
1	0.2	0.05	-0.25	-0.3	-0.25	-0.3	-0.25	-0.05
2	-0.25	-0.3	-0.25	0.05	0.2	0.05	-0.25	-0.3
3	-0.25	0.05	0.2	0.05	-0.25	-0.3	-0.25	-0.3
4	-0.25	-0.3	-0.25	-0.3	-0.25	0.05	0.2	0.05
The angle of the roof is $<10^\circ$								
Front	-0.5	-0.5	-0.4	-0.5	-0.5	-0.5	-0.4	-0.5
Back	-0.5	-0.5	-0.4	-0.5	-0.5	-0.5	-0.4	-0.5
The angle of the roof is $11^\circ-30^\circ$								
Front	-0.3	-0.4	-0.5	-0.4	-0.3	-0.4	-0.5	-0.4
Back	-0.3	-0.4	-0.5	-0.4	-0.3	-0.4	-0.5	-0.4
The angle of the roof is $>30^\circ$								
Front	0.25	-0.3	-0.5	-0.3	-0.4	-0.3	-0.5	-0.3
Back	-0.4	-0.3	-0.5	-0.3	0.25	-0.3	-0.5	-0.3

Table 2 The C_p values on difference surfaces of a building like Fig. 6 [29]

Surface	C_p values, wind direction α							
	0	45	90	135	180	225	270	315
(a) Without block (the building is located in an open area)								
1	0.5	0.25	-0.5	-0.8	-0.7	-0.8	-0.5	-0.25
2	-0.7	-0.8	-0.5	0.25	0.5	0.25	-0.5	-0.8
3	-0.9	-0.2	0.6	0.2	-0.9	-0.6	-0.35	-0.6
4	-0.9	-0.6	-0.35	-0.6	-0.9	0.2	0.6	0.2
The angle of the roof is $<10^\circ$								
Front	-0.7	-0.7	-0.8	-0.7	-0.7	-0.7	-0.8	-0.7
Back	-0.7	-0.7	-0.8	-0.7	-0.7	-0.7	-0.8	-0.7
The angle of the roof is $11^\circ-30^\circ$								
Front	-0.7	-0.7	-0.7	-0.6	-0.5	-0.6	-0.7	-0.7
Back	-0.5	-0.6	-0.7	-0.7	-0.7	-0.7	-0.7	-0.6
The angle of the roof is $>30^\circ$								
Front	0.25	0	-0.6	-0.9	-0.8	-0.9	-0.6	0
Back	-0.8	-0.9	-0.6	0	0.25	0	-0.6	-0.9
(b) With some block (the building is located in an open area with some lower constructions around)								
1	0.25	0.06	-0.35	-0.6	-0.5	-0.6	-0.35	0.06
2	-0.5	-0.6	-0.35	0.06	0.25	0.06	-0.35	-0.6
3	-0.6	0.2	0.4	0.2	-0.6	-0.5	-0.3	-0.5
4	-0.6	-0.5	-0.3	-0.5	-0.6	0.2	0.4	0.2
The angle of the roof is $<10^\circ$								
Front	-0.6	-0.6	-0.6	-0.6	-0.6	-0.6	-0.6	-0.6
Back	-0.6	-0.6	-0.6	-0.6	-0.6	-0.6	-0.6	-0.6
The angle of the roof is $11^\circ-30^\circ$								
Front	-0.6	-0.6	-0.55	-0.55	-0.45	-0.55	-0.55	-0.6
Back	-0.45	-0.55	-0.55	-0.6	-0.6	-0.6	-0.55	-0.55
The angle of the roof is $>30^\circ$								
Front	0.15	-0.08	-0.4	-0.75	-0.6	-0.75	-0.4	-0.08
Back	-0.6	-0.75	-0.4	-0.08	-0.15	-0.08	-0.4	-0.75
(c) With block (the building is located in downtown area with high constructions around)								
1	0.06	0.12	-0.2	-0.38	-0.3	-0.38	-0.2	-0.12
2	-0.3	-0.38	-0.2	0.12	0.06	0.12	-0.2	-0.38
3	-0.3	0.15	0.18	0.15	-0.3	-0.32	-0.2	-0.32
4	-0.3	-0.32	-0.2	-0.3	-0.3	0.15	0.18	0.15
The angle of the roof is $<10^\circ$								
Front	-0.49	-0.46	-0.41	-0.46	-0.49	-0.46	-0.41	-0.46
Back	-0.49	-0.46	-0.41	-0.46	-0.49	-0.46	-0.41	-0.46
The angle of the roof is $11^\circ-30^\circ$								
Front	-0.49	-0.46	-0.41	-0.46	-0.4	-0.46	-0.41	-0.46
Back	-0.4	-0.46	-0.41	-0.46	-0.49	-0.46	-0.41	-0.46
The angle of the roof is $>30^\circ$								
Front	0.06	-0.15	-0.23	-0.6	-0.42	-0.06	-0.23	-0.15
Back	-0.42	-0.6	-0.23	-0.15	0.06	-0.15	-0.23	-0.6

Fig. 5 Sketch map of a three-story-high square building

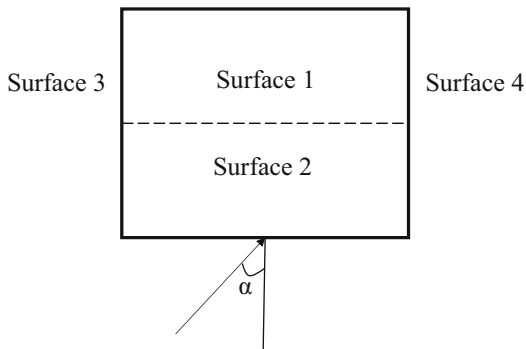


Fig. 6 Sketch map of a three-story-high rectangle building with 2:1 aspect ratio

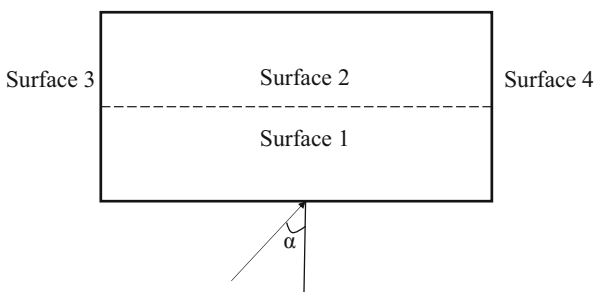
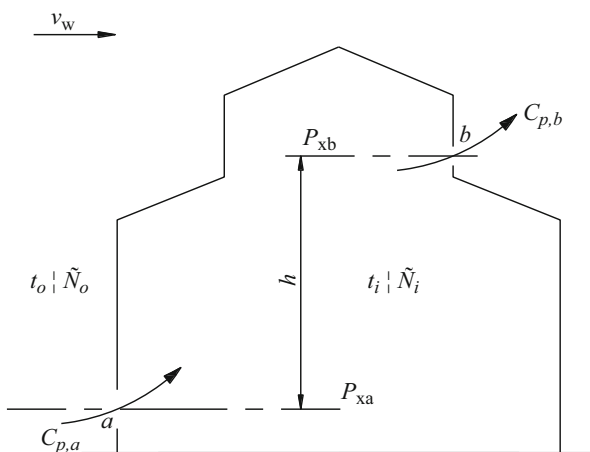


Fig. 7 Natural ventilation driven by wind and buoyancy



parameters in each room are equally distributed, yet it is not suitable for predicting the airflow distribution within the building. Nowadays, many software tools such as CONTAMW, SPARK, COMIS, EnergyPlus, DOE-2, MIX, and DEST are developed based on multi-zone model to predict airflow and temperature distribution. The

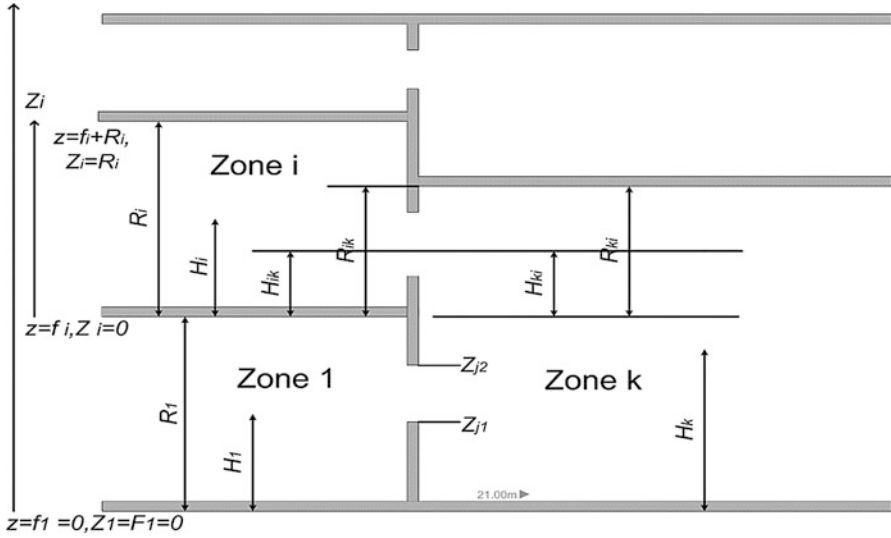


Fig. 8 Geometric definition of zones and openings in MIX model

general steps of using the software tools include the establishment of building models, the determination of initial parameters, and the calculation of results.

As pressure differences are the fundamental causes of airflow through zones, the MIX (Multi-zone Infiltration and eXfiltration) model developed by Li [7] is based on the calculation of pressure differences between different zones. Pressure differences are resulted from buoyancy and wind, and bidirectional flow in each opening is considered. Air temperature in all zones is assumed to be uniform and is regarded as known parameters for simplification of the model.

Good geometry data management is conducive to implying the calculation process of the pressure difference and flow rate equations; thus code efficiency can be improved [7]. A proposed geometry data representing method is shown in Fig. 8. The building is divided into N zones, and the outdoor is taken as Zone 0. The basic zone division rule is that each boundary either separates two zones with significant air temperature difference or provides significant flow resistance. Two coordinate systems are used, respectively, a global coordinate and a local coordinate. The global vertical coordinate z is chosen for the entire building, and the origin of z is at the ground level of Zone 1. The lowercase letters such as r_i , h_i , and f_i represent the ceiling height, middle height, and floor height of Zone i in global vertical coordinate, respectively. The local coordinate z' is chosen for each zone considered. The origin of z' is at the floor level of the zone. The capital letters such as R_i , H_i , and F_i represent the ceiling height, middle height, and floor height of Zone i in local vertical coordinate, respectively. $Z_i = z - f_i$. In general, $F_i = 0$. $R_i = r_i - f_i$, $H_i = h_i - f_i$.

For a vertical opening at height z , the pressure difference between Zone i and Zone 0 can be obtained as

$$\Delta p_{\text{tot}}(z) = \frac{1}{2}\rho_0 C_p(z)v^2(z) - g \int_{h_i}^z (\rho_0 - \rho_i) dz - (p_{0i} - p_{00}) - \rho_0 g(h_i - h_1) \quad (19)$$

where ρ_0 is the air density in Zone 0 (kg/m³), ρ_i is the air density in Zone i (kg/m³), C_p is the wind pressure coefficient on the building surface, v is wind speed (m/s), and g is the gravitational acceleration (m/s²). A positive pressure difference always indicates inflow to Zone i as a convention. The term $(p_{0i} - p_{00})$ is defined as the zonal internal pressure, p_i , at the height $H_i(h_i)$ relative to the ambient pressure at the datum level $H_1(h_1)$.

The ventilation rate of Zone i through opening j is $q_{j,i}$:

$$q_{j,i} = K_t A (|\Delta p_{\text{tot}}|)^n \text{sgn}(\Delta p_{\text{tot}}) \quad (20)$$

where K_t is the flow coefficient which is determined by the shape, size, and permeability of the openings and A is the area of the opening. For the sake of simplicity, n is taken as 0.6 for small openings. If the equation is also used for large openings, $K_t = C_d \sqrt{2/\rho}$ and $n = 0.5$ [7]. Take the derivative with respect to z , Eq. (29) can be deduced as

$$dq = K_t b (|\Delta p_{\text{tot}}|)^n \text{sgn}(\Delta p_{\text{tot}}) dz \quad (21)$$

where b is the opening width. The airflow through all zones in the same building (a control volume) conforms with mass conservation equation. Therefore,

$$\sum_{j=1}^{N_i} q_{j,i} + q_s + q_e = 0 \quad (22)$$

where N_i is the number of all the openings and q_s and q_e represent the air supply rate and exhaust rate of mechanical ventilation, respectively, if the calculated building is hybrid-ventilated. Each zone has a set of differential equations of the internal pressure differences p_i if Eqs. (21) and (22) are combined together. Then, the internal pressure differences can be solved, and the same is the ventilation rate of each opening.

Computational Fluid Dynamics (CFD) Model

Computational fluid dynamics (CFD) model, also considered as numerical simulation model based on computers, achieves the purpose of solving engineering problems and physical problems by using numerical calculation and image display. The basic principle is to use a large number of grids to divide the model space into many tiny regions, solving the differential equations, governing the flow of the fluid by

numerical method, and gaining the discrete distribution of the flow parameters in the continuous region. The numerical simulation method can provide the concrete details of the fluid flow in the space, such as the time-varying characteristics of velocity field, pressure field, and temperature field distribution, making the traditional building thermal environment research and design process evolve. At the same time, the numerical simulation method can accurately predict the overall ventilation performance and environmental parameters of the study object, which is easy to find the engineering design problems from the analysis process. It only needs to be recalculated once to determine whether the improvement is effective or not. Moreover, it is easier to obtain some regular knowledge based on this proposed improvement program. During the period of thermal environment research, design, and optimization, the dependence of the experiment and experience is greatly reduced which can significantly shorten the experimental cycle and reduce costs.

The commonly used CFD softwares include Phoenix, Fluent, CFX, FloVENT, CFX, STAR-CD, etc. Fluent and Phoenix are more commonly used in the field of ventilation and air conditioning. Phoenix has a great advantage in modeling the interface with the outside world. The spatial model of the simulation object can be created through using 3D MAX and CAD tools and then imported into the analysis domain through the Phoenix input interface. Airpak, a software developed by Fluent Corporation toward engineers, , and designers, which is professionally applied to the HVAC field, can accurately simulate the air flowing, air quality, heat transfer, contamination, and comfort of the ventilation system. It is optimized for modeling, meshing, and post-processing. In comparison with Fluent software, Airpak is more convenient to use and more suitable for those architects and engineers who do not know much about CFD technology and fluid mechanics.

Application of computational fluid dynamics in building ventilation uses numerical methods to solve the partial differential equations of momentum, energy, and mass. The air temperature, pressure, airflow rate, water vapor pressure, and pollutant concentration can be obtained from solving the CFD model. Using the CFD model to simulate the ventilation process demands users' professional ability and the high performance of the computer. CFD model is extensively used in the study of indoor air quality, thermal comfort, fire protection, and air conditioning systems. Compared with other models, CFD model is the most commonly used analysis method. There are many kinds of CFD software for wind environment analyzing.

After adequately understanding the project requirements and the simulation purpose, general principles must be followed to ensure reliability of computer simulation. Besides, the geometric model size of the physical model should be constructed in accordance with the actual building size 1:1 and should include the key components. Physical model should also be simplified on the premise of not significantly affecting the physical quantity of the object. In addition, the symmetry plane can be set according to the symmetry of the model and boundary conditions.

The computational domain should be determined on the basis of the building geometry. When using the indoor and outdoor joint simulation method, the computational horizontal length and width should be greater than five times the building height, and the calculation domain of the vertical direction should be greater than

four times the building height. Beyond that, the usage of indoor and outdoor step-by-step simulation method should follow the wind environment simulation requirements.

To construct the physical model, the model of doors, windows, and other ventilation openings of the building should base on the common opening and closing situation, and the open area of natural ventilation should be set according to the actual openable area. Moreover, the modeling of the interior space of the target building should be established with all indoor partitions, which should contain large cabinets, but do not include some furniture such as tables and chairs.

Based on the previous workers' experience, the method of indoor and outdoor joint simulation should adopt multi-scale grid, the indoor grid should be able to reflect all the significant barrier ventilation of the indoor facilities, and the grid transition ratio should not be greater than 2. When using indoor and outdoor step-by-step simulation methods, the indoor grid should be able to reflect all the significant barrier ventilation of the indoor facilities, and the ventilation port should have 9 (3×3) or more of the grid.

According to the characteristics of the calculated objects and the purpose of calculation, the appropriate turbulence model is selected. The commonly used turbulence models include standard $k-\varepsilon$ model, RNG $k-\varepsilon$ model, and LES model.

Before calculation, it is necessary to input reasonable boundary conditions regardless of steady and nonsteady simulation. There is a unified set of basic boundary conditions for outdoor condition. The basic boundary conditions for warm environment simulation include outdoor wind speed, wind direction, and outdoor air temperature. Besides, the basic boundary conditions should be determined based on the measured value of the project site and the purpose of the simulation. Regarding indoor boundary conditions, natural ventilation simulation does not have to consider the indoor thermal boundary conditions for the space with height ≤ 5 m or volume $\leq 10,000$ m³. Besides, thermal boundary conditions should be set reasonably when analyzing the indoor thermal environment as a simulation target or the court space is greater than the above criteria. Additionally, other physical parameters such as density, thermal conductivity, and specific heat capacity should be defined. Iterative time and other necessary calculation control parameters are input ultimately.

The results obtained from CFD can be displayed in the form of figures and tables by post-processing software, such as Tecplot and Origin.

The Influence of Porous Screens on Ventilation Rate

Most buildings in China use porous screens on openings to prevent insects and particles. As porous screens provide an extra resistance for mass, momentum, and heat transport, the natural ventilation rate and efficiency are inevitably changed by porous screens [30].

For one-dimensional, steady-state airflow through a permeable material, the motion equation can be expressed as follows [31]:

$$\begin{aligned}
 (\rho/\varepsilon^2)u(\partial u/\partial x) &= -\partial P/\partial x - (\mu/K)u - \rho(Y/K^{1/2})|u|u \\
 &+ (\mu/\varepsilon)(\partial^2 u/\partial x^2)
 \end{aligned}
 \tag{23}$$

with $u = \varepsilon u_i$, where u is the superficial fluid velocity (m/s), u_i the velocity through the material (m/s), ρ the density of air (kg/m^3), P the pressure (Pa), x the flow direction, K the permeability of the medium (m^2), ε the porosity, and Y the inertial factor. For highly porous materials, Reynolds number ($\text{Re}_i = \frac{u_i d_{\text{bore}}}{\nu}$, where d_{bore} is the diameter of the bore) smaller than 100 to 150, the convective inertia effects $((\rho/\varepsilon^2)u(\partial u/\partial x))$, and viscous resistance of fluid flow $((\mu/\varepsilon)(\partial^2 u/\partial x^2))$ can be ignored, while the pore inertia effects $(\rho(Y/K^{1/2})|u|u)$ and viscous resistance force caused by the momentum transfer at matrix-fluid interface $((\mu/K)u)$ cannot be ignored [30]. Equation (23) reduces the Forchheimer equation:

$$(\mu/K)u + \rho(Y/K^{1/2})|u|u = -\partial P/\partial x
 \tag{24}$$

The permeability K and inertial factor Y can be derived by fitting the experimental data of pressure drops as a second-order polynomial. A.F. Miguel [31] performed measurements on 14 different screen samples and found the best fitted equations of K and Y as follows:

$$K = 3.44 \times 10^{-9} \varepsilon^{1.6}, Y = 4.30 \times 10^{-2} / \varepsilon^{2.13}
 \tag{25}$$

which is valid for $0.04 \leq \varepsilon \leq 0.90$. D.L Valera [32] measured the screen thickness by conducting an analysis images system and gave the different correlation equations as

$$K = 5.68 \times 10^{-8} \varepsilon^{3.68}, Y = 5.67 \times 10^{-2} / \varepsilon^{1.1604}
 \tag{26}$$

with $0.288 \leq \varepsilon \leq 0.483$.

For Re_i bigger than 100 to 150, the convective inertia effects $((\rho/\varepsilon^2)u(\partial u/\partial x))$ cannot be ignored, while the viscous resistance force caused by the momentum transfer at matrix-fluid interface $((\mu/K)u)$ can be ignored. Equation (23) reduces to

$$(\rho/\varepsilon^2)u(\partial u/\partial x) = -\partial P/\partial x - \rho(Y/K^{1/2})|u|u
 \tag{27}$$

The integration of Eq. (27) yields to the Bernoulli-type equation:

$$\Delta P = \frac{1}{2} F_{O,S} \rho u^2, F_{O,S} = F_O + F_S
 \tag{28}$$

where $F_{O,S}$ is the loss coefficient of the screened opening, F_O the loss coefficient for the unscreened opening, and F_S the loss coefficient of the screen. B.J. Bailey [33] performed experiments on five insect screens and obtained a screen loss coefficient equation:

$$F_s = \left[\frac{18}{\text{Re}} + \frac{0.75}{\log(\text{Re} + 1.25)} + 0.055 \log(\text{Re}) \right] \left[\frac{1 - \varepsilon^2}{\varepsilon^2} \right] \quad (29)$$

with $\text{Re} = \frac{u d_{\text{yam}}}{\nu}$, where d_{yam} is the diameter of the yarn.

Equations (24, 25, 26, 27, 28, and 29) can be used to calculate the resistance caused by porous screens and finally calculate the ventilation rate through screened openings.

Measurement of Natural Ventilation Rate

Tracer Gas Method

As the frequency spectrum of natural ventilation varies frequently, the heat source, temperature difference, opening strategy, wind speed, direction, etc. can make an influential impact on the ventilation rate, airflow distribution, and direction. Tracer gas method is the most reliable way to obtain the natural ventilation rate.

Tracer gas method is the process of releasing a small amount of tracer gas into the measured room (or building) and recording its concentration varying with time. Subsequently, the ventilation rate can be calculated from the obtained data based on appropriate evaluation algorithms. During the measurement, the air is considered to be completely mixed with no concentration gradients existing inside the room. The measured room or building is considered as a single-zone system. Ideally, air exchange only occurs between the tracer gas-containing air and the ambient air. The air exchange with other interior spaces is thought to be negligible. The ventilation rate is assumed to be constant during the measurement. Thus, the ventilation rate can be modeled by the mass balance equation, as shown in Eq. (30):

$$\begin{cases} \frac{dC_{\text{in},t}}{dt} = n(C_{\text{out}} - C_{\text{in}}) + \frac{E}{V} \\ C_{\text{in},\tau} = C_{\text{in},0}, t = 0 \end{cases} \quad (30)$$

where t represents time (h), $C_{\text{in},t}$ is the tracer gas concentration inside the room at the time t (ppm or $\mu\text{g}/\text{m}^3$), $C_{\text{in},0}$ indicates the tracer gas concentration inside the room at the time $t = 0$ (ppm or $\mu\text{g}/\text{m}^3$), C_{out} is the tracer gas concentration at outside (ppm or $\mu\text{g}/\text{m}^3$), V is the volume of the measured room (m^3), n is the air change rate (1/h or ACH), and E is the tracer gas's emission rate during the measurement (m^3/h).

Equation (30) can be characterized by the following features: If no tracer gas is emitted into the room (i.e., $E = 0$) and a non-zero tracer gas $C_{\text{in},0}$ is already presented at the $\tau = 0$ which is higher than the outdoor air concentration C_{out} , the exact solution of Eq. (30) can be expressed as follows:

$$C_{\text{in},t} = (C_{\text{in},0} - C_{\text{out}}) \exp(-nt) + C_{\text{out}} \quad (31)$$

If the tracer gas concentration outside is zero (i.e., $C_{out} = 0$), Eq. (31) can be simplified as

$$C_{in,t} = (C_{in,0})\exp(-nt) \tag{32}$$

If the tracer gas is emitted at a constant rate E and the initial tracer gas concentration inside the room is equal to that at outside ($C_{in,0} = C_{out}$), the tracer gas will accumulate within the room, and the exact solution of Eq. (32) can be expressed as

$$C_{in,t} = \frac{E}{nV}(1 - \exp(-nt)) + C_{out} \tag{33}$$

For $t \gg 1/n$, the final equilibrium indoor concentration will be achieved, and Eq. (34) can be simplified as

$$C_{eq} = \frac{E}{nV} \tag{34}$$

where C_{eq} is the equilibrium concentration. Equations (31), (32), (33), and (34) form the basis for determining the air change rate with tracer gas measurements under different conditions. According to Laussmann and Helm [5], the concentration decay method, the constant injection method, and the constant concentration method are three existing methods which are appropriate for the determination of air change rate with the use of tracer gas.

Concentration Decay Method

Concentration decay method is the process of injecting a small amount of tracer gas into the room at first and recording the indoor tracer gas concentration with regular time intervals after the tracer gas is well-mixed. The concentration decay curve follows an exponential decay tendency (as shown in Eq. 31). The nominal time constant ($\tau = 1/n$) is defined as the time when the air change cycle is completed [34]. After the time period $\tau(1/n)$ and $3\tau(3/n)$, there will be $\approx 37\%$ ($100/e^1$) and $\approx 5\%$ ($100/e^3$) old room air left, respectively. It should be noticed that the total time interval between the first and the last calculation points should be in the order of magnitude of the nominal time constant τ [34, 35]. Table 3 presents recommendation of the minimum time spans between the first and last sampling and the corresponding sampling interval.

The air change rate can be determined by using Eq. (31) and nonlinear regression analysis, as shown in Fig. 9a. In most cases, a linear relationship between tracer gas concentration and the time t is used, which can be found in Eq. (35):

$$\ln\left(\frac{C_{in,0} - C_{out}}{C_{in,\tau} - C_{out}}\right) = nt(+b) \tag{35}$$

where b is the intercept term of linear fit; see Fig. 8b. If there are only a few sampling values available, e.g., the sampling is performed with syringes or other appropriate methods, the air change rate can be calculated by Eq. (36):

Table 3 Recommendation of minimum time spans between the first and last sampling and the corresponding sampling interval for air change measurement using tracer gas decay method [5, 34]

Air change rate (ACH)	Minimum time span of tracer gas measurement (h)	Air change rate (ACH)	Sampling interval (min)
0.05	20		
0.125	8		
0.25	4	<0.5	30–40
1	1	0.5–1	20–30
2	0.5	1–2	10
4	0.25	2–5	5
10	0.1	>10	<2

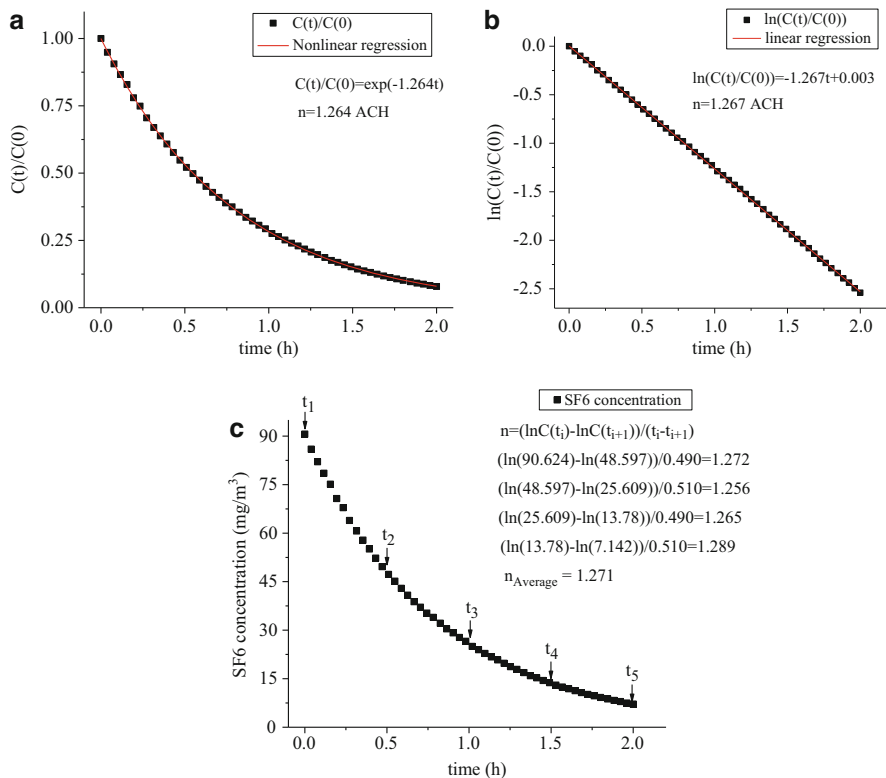


Fig. 9 Air change rate determined from tracer gas decay method. (a) Nonlinear regression method; (b) linear regression method; and (c) two-point method

$$n = \ln \left(\frac{C_{in,t(i)} - C_{out}}{C_{in,t(i+1)} - C_{out}} \right) / \left((t_{i+1}) - t(i) \right) \tag{36}$$

where $C_{in,t(i)}$ is the indoor tracer gas concentration at time $t(i)$ and $t(i + 1) - t(i)$ is the time interval between two measured points. This method is called the two-point method, as presented in Fig. 9c. Among them, the linear regression method is more recommended.

The concentration decay method is the most commonly used one in practice [5] as it is easy to operate, the needed amount of tracer gas is low compared with constant injection method, and the results are relatively reliable. However, it cannot reflect the timely fluctuation of ventilation rate as it assumes that the ventilation rate is constant during the measurement.

Constant Injection Method

Constant injection method is the process that a certain amount of tracer gas is constantly released during the measurement. The indoor tracer gas concentration increases with time and finally reaches the equilibrium concentration. As a result, the constant injection method is also called step-up method [36]. According to Eq. (36), the equilibrium concentration depends on the measured room volume V , the air change rate n , and the emission rate E , which can be used to calculate the air change rate n . As it takes a long time to reach the equilibrium concentration, constant injection method is time-consuming and tracer-gas-consuming. If the equilibrium is not measured, the curve has to be extrapolated by nonlinear regression to determine this value, causing unavoidable fitting errors.

Constant Concentration Method

Constant concentration method is the process of keeping the indoor tracer gas concentration a predefined value, monitoring and controlling the indoor tracer gas concentration based on an automated dosing and control system. In this case, the ventilation rate is proportional to the tracer gas supply rate, and the ventilation rate can be calculated from the ratio of tracer gas supply to the tracer gas concentration [5]. This method has an advantage over detecting the ventilation rate timely, and even short-term changes of ventilation rate can be measured. However, the high-cost equipment and operation make this method be rarely used for indoor air quality evaluation.

Tracer Gases

To ensure that the tracer gas can be completely mixed with the indoor air and is diluted by the outdoor fresh air only, some requirements for tracer gas need to be satisfied. Firstly, the tracer gas should have stable physical and chemical properties, avoiding adsorption by the building or furniture surfaces, dissolution in the water, and chemical reactions with components in the indoor air. Secondly, the tracer gas density should be close to the air density to be easily mixed up and freed from concentration stratification. Thirdly, the tracer gas should be nontoxic, nonflammable, and environmentally friendly. Fourthly, the tracer gas concentration in air should be zero or constant naturally. Last but also importantly, the tracer gas should be easily available at a reasonable cost.

Table 4 A comparison of the three commonly used tracer gases [36]

Tracer gas	Density (Air is 1.2 kg/m ³)	Toxicity, threshold value	Background concentration	Cost
SF ₆	6.3	1000 ppm	0	50 €/kg
CO ₂	1.9	5000 ppm	400–450	Cheap
N ₂ O	1.9	50–100 ppm	0	15 €/kg

The most actually used tracer gases are N₂O (nitrous oxide, also known as laughing gas) and SF₆ (sulfur hexafluoride). Besides, CO₂ could also be used when the background concentration is constant [36]. Some properties of them are shown in Table 4. As SF₆ is heavier than air, it should be mixed with the room air continuously as it is supplied or premixed with carrier gas before emission. In addition, its cost is relatively high. The density of CO₂ is close to air, but its background concentration in ambient air is 400–450 ppm and could be influenced by CO₂ emitted by human's metabolism. Therefore, CO₂ can only be used when the influence by human beings can be avoided and the background concentration is stable. N₂O avoids the disadvantages of the first two. As a result, when the indoor concentration is not beyond the threshold and the measurement conditions are permitted, N₂O is more suitable than SF₆ and CO₂ [36].

Air Velocity Measuring Method

Air velocity measuring method is always used to measure the mechanical ventilation rate as the airflow through ducts and air inlets is more stable than natural ventilation. Since the wind frequency and turbulence intensity in naturally ventilated conditions are higher than those in mechanically ventilated conditions, the air velocity measuring method is little used in measuring natural ventilation rate, but it is always used to analyze the airflow distribution as it can reflect the difference of air velocity at different places.

Natural Ventilation Form

General Natural Ventilation Form

Buoyancy-Driven Ventilation

Single-side ventilation, which is the most common type of buoyancy-driven ventilation, is the process that natural ventilation enters and exits a room through openings on a single side according to Fig. 10a, b. Single-side ventilation mainly relies on the turbulence of air and buoyancy pressure between the inside and the outside to exchange air. In general, the ventilation rate is lower than cross-ventilation. The higher the height between the opening and the neutral plane, the higher the

ventilation rate of single-side form. Therefore, chimney effect is an instructive way to enhance the buoyancy-driven ventilation performance.

Wind-Driven Ventilation

Wind-driven ventilation uses the force of the wind to ventilate air through the building. According to Fig. 11, cross-ventilation is the most common form of wind-driven ventilation. It refers to that the airflow inlet and outlet are on the opposite walls, respectively, and the natural ventilation can pass through the whole room from the inlet to the outlet, as shown in Fig. 10. If there is an obstacle (e.g., screen) between the air inlet and outlet, the wind will be blocked, and the ventilation effect will be significantly reduced. Generally, the distance between air intake and outlet should be 2.5–5 times the height of the roof (about 6.5 m). Generally, cross-

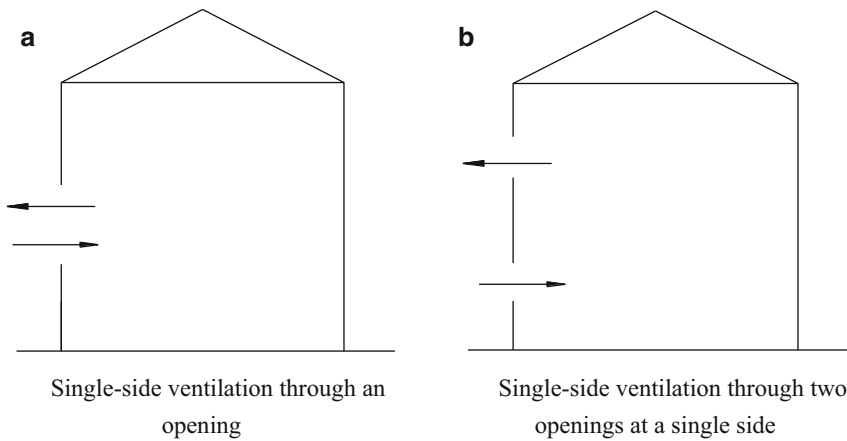
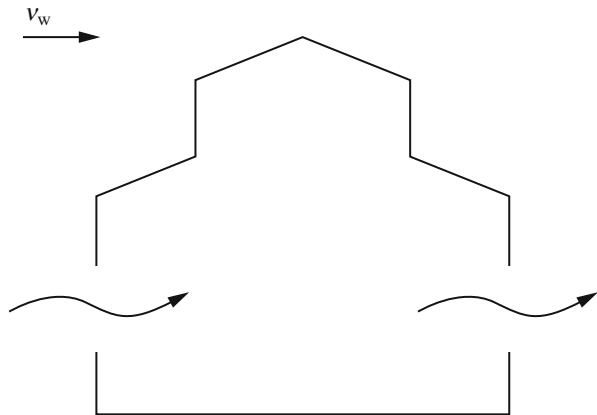


Fig. 10 Single-side ventilation. (a) Single-side ventilation through an opening. (b) Single-side ventilation through two openings at a single side

Fig. 11 Cross-ventilation



ventilation is easy to achieve in rooms with small depth. For large buildings, methods such as courtyard, atrium, and corridor can be used to strengthen cross-ventilation. Wind-driven ventilation is unreliable as it is dependent on the climate conditions and buoyancy-driven ventilation can act as an assistant.

Methods to Enhance the Natural Ventilation Performance

There are numerous ways which can be used to improve the natural ventilation performance. For example, stack effect can be applied to enhance the buoyancy-driven ventilation, and cross-ventilation can make full use of the wind-driven pressure with rational geometry configuration of buildings. As the utilization of wind-driven pressure highly depends on the outdoor meteorological conditions, the methods to enhance buoyancy-driven ventilation are more reliable and more frequently used. The common ways to improve buoyancy-driven ventilation performance include atrium ventilation, solar chimneys, and so on. Ventilation cap is often applied to improve the wind-driven ventilation performance. Moreover, wind-proofed skylight is used to guide the airflow direction and ensure the skylight acting as an outlet.

Atrium Ventilation

Atrium is a kind of building component that is often used in modern office buildings, which can not only bring outdoor light into the room but also can play the role in natural ventilation. As shown in Fig. 12, atrium ventilation utilizes the temperature gradient in the vertical direction of the vertical cavity in the building and the indoor and outdoor temperature difference to drive natural ventilation by the buoyancy pressure between the upper and the lower openings. Besides, the atrium ventilation is also called “the chimney effect.”

According to the Bernoulli equation, the ventilation rate is directly proportional to the height difference between the openings, indicating the ventilation rate increases with the increase of the height difference when the temperature difference remains constant. The ventilation rate is also related to indoor and outdoor temperature difference. In general, the greater the temperature difference, the greater the

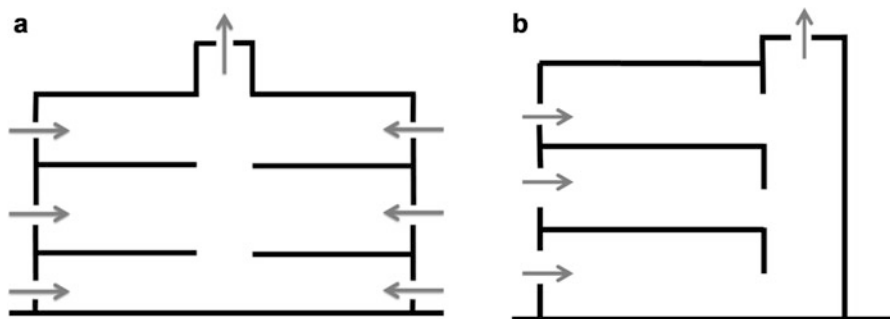


Fig. 12 Atrium ventilation

ventilation rate. Many public buildings use this strategy to enhance ventilation. With mechanical devices sucking the outdoor fresh air and the dome absorbing solar energy, “chimney effect” is used to exhaust the indoor air from the top of the room.

Solar Chimney

As presented in Fig. 13, the solar chimney is a kind of enhanced natural ventilation equipment that can convert thermal energy into kinetic energy. To provide the buoyancy of airflow, it uses solar radiation as the power and utilizes the density difference. This technology has been applied to the construction of heating, ventilation, and solar rooms in Europe, the United States, and some Asian countries. Solar chimney can be divided into three categories, respectively, vertical solar chimney, inclined solar chimney, and Trombe wall solar chimney. Table 5 shows the performance of different solar chimneys.

Nowadays, the research of solar chimneys at home and abroad mainly bases on theory, experiments, and numerical simulation methods. It can be found that the ventilation performance of solar chimney relates to wall structure, physical property, solar radiation intensity, meteorological parameters, etc. Optimization of solar chimney can create a green, energy-saving, and comfortable living environment for human beings.

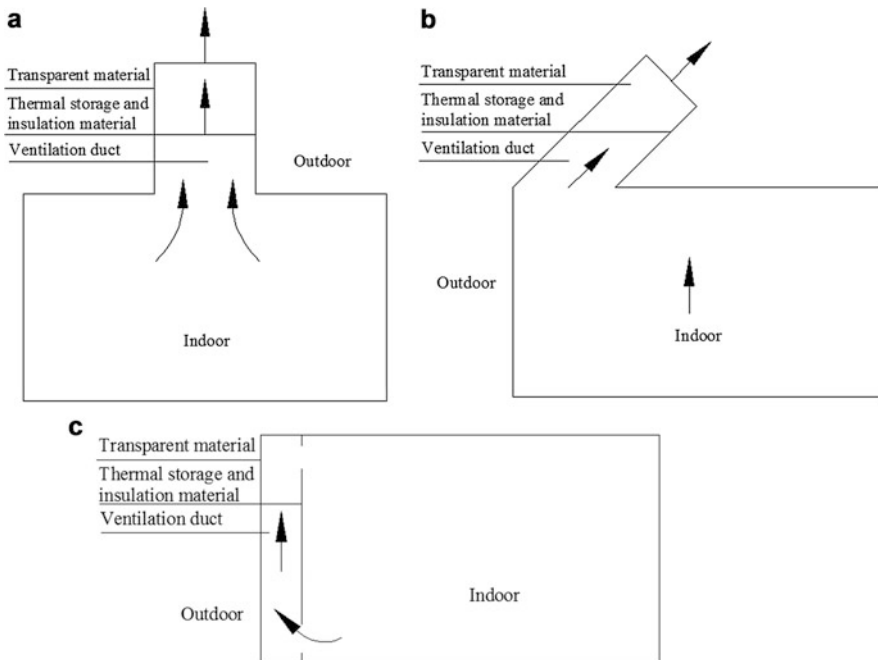
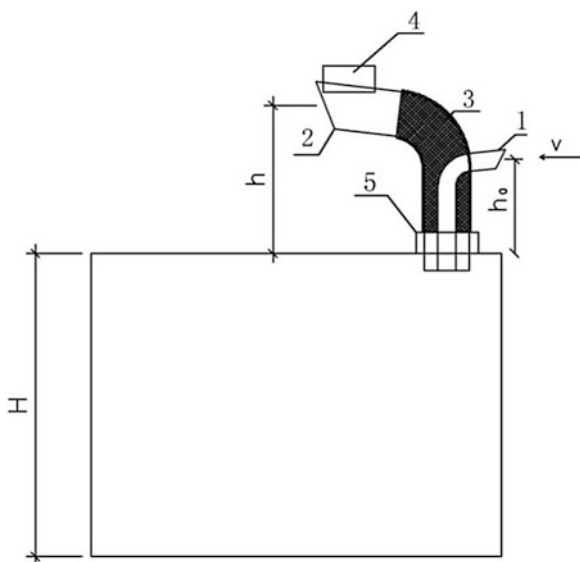


Fig. 13 Solar chimney

Table 5 The performance of different solar chimneys

Forms	Advantages	Disadvantages
Vertical solar chimney	Simple structure, good matching with buildings, and easy to install	The pressure loss inside the chimney is relatively large, and the optimal depth-to-height ratio of the chimney is not ideal or does not exist
Inclined solar chimney	The pressure loss inside the chimney is small, the velocity distribution is uniform, and the ventilation rate is large	The inclined angle determines the performance of chimney, and the installation is complicated
Trombe wall solar chimney	Supply heat in winter and the best depth ratio and easy to achieve	Backflow phenomenon and large pressure loss

Fig. 14 Ventilation cap with auto-modified inlet. 1 air inlet duct; 2 air outlet duct; 3 solar heat-collection plate; 4 wind cap; 5 bearing



Ventilation Cap

According to Fig. 14, ventilation cap is a kind of natural ventilation attachment that is often applied in large workshops, basements, etc. This technology adopts wind-driven pressure and buoyancy pressure to capture the natural wind. The effect of buoyancy pressure should be consistent with the effect of wind-driven pressure, so the ventilation performance can be enhanced. Solar energy can be used to strengthen the buoyancy pressure effect. The ventilation cap with auto-modified inlet has been invented, as shown in Fig. 14. The auto-modified ventilation cap makes use of both wind pressure and buoyancy pressure provided by solar-thermal materials to drive airflow through the building; thus the bidirectional ventilation can be realized. It consists of the air inlet duct and outlet duct, solar-thermal materials, wind cap, and bearings. When wind blows, the wind cap would be under pressure so that the direction of inlet duct can be adjusted to

Fig. 15 Skylight with windshields

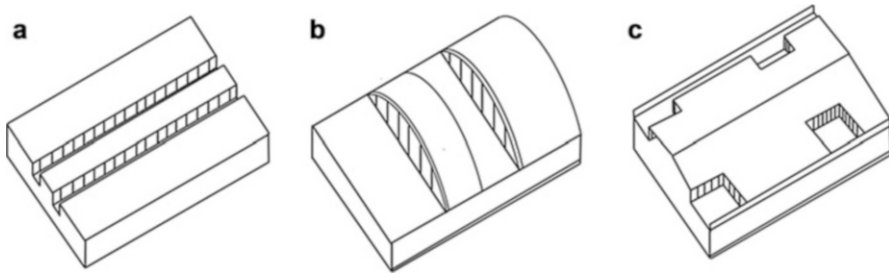
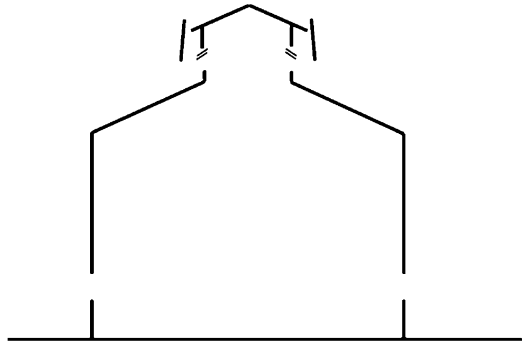


Fig. 16 Skylight. (a) Vertical sunk skylight. (b) Horizontal sunk skylight. (c) Patio skylight

face the wind by the bearing at the bottom of the ventilation cap. At the same time, the solar-thermal materials will increase the temperature inside the air outlet duct and help exhaust. Obviously, factors such as the outdoor wind speed, the air temperature in the air outlet duct, and the vent size can make a great influence on the ventilation rate. The performance of ventilation cap can be optimized according to the change of factors. Besides, the pressure drop between the air inlet duct and outlet duct and the outdoor air quality should be considered in the practical application.

Wind-Proofed Skylight

In natural ventilation buildings with skylights, the excess heat and some harmful gases need to be discharged through the skylights to the outside. This requires that the skylight have a good exhaustion performance, indicating that the airflow cannot enter the building from the skylight in any climate conditions. For ordinary skylights, wind always blows into the skylight on the windward side. Under such conditions, the predefined airflow distribution inside the building will be destroyed. Therefore, windshields are often used in these skylights in order to prevent the air from flowing back, which can be found in Fig. 15. The space between the windshield and the sash of the skylight is 1.0–1.5 times the height of the skylight. There is a gap of 50–100 mm between the windshield’s lower edge and the roof for draining. Both ends of the windshield are sealed to prevent in the flow of wind. Several common skylights are shown in Fig. 16a–c.

Design for Natural Ventilation

The calculation of natural ventilation can be categorized into the design calculation and the checking calculation. The design for natural ventilation is the process of determining the ventilation strategies and the opening positions according to the predefined indoor temperature and ventilation rate. To meet the predefined conditions, the checking calculation is necessary to analyze whether the ventilation rate and indoor temperature is qualified or not.

There are three elements for the design of ventilation. At first, the ventilation rate must be large enough to meet the current standards or guidelines. Secondly, air should flow from clean areas to unclean areas. Thirdly, the indoor airflow distribution should be uniform and avoided from blind corners.

The design for natural ventilation involves three basic steps [37]. Firstly, the desired airflow pattern and the driving forces from the inlet openings to the outlet openings need to be determined. This step is associated with the building's form (single-side corridor, central corridor, wind tower, etc.) and organization (relative location of kitchen room, bathroom, etc.). Secondly, the suitable ventilation rate to remove indoor pollutants and indoor thermal load should be identified. The ventilation rate and indoor thermal load play a determining role in selecting vent size and locations. Thirdly, the sizes and locations of openings can be calculated in accordance with the previous steps.

General Procedure for Natural Ventilation Design

A number of factors such as thermal comfort, indoor air quality, and fire safety need to be considered for the design of naturally ventilated buildings. Other unfavorable ambient environment factors such as noise and air pollution need to be assessed before the building design starts.

Thermal comfort in naturally ventilated building is different from that in mechanically ventilated building. To predict the thermal comfort in naturally ventilated buildings, ASHARE Standard 55–2010 [38] developed a thermal comfort model according to the field-measured database of 21,000 office buildings. The results are shown in Fig. 17. The acceptable indoor operative temperature is centered at the neutral temperature. Besides, the acceptable temperature width is ± 5 °C of the neutral temperature for 90% occupants and ± 7 °C for 80% occupants. The 80% acceptability limits can be considered as typical limits, while the 90% acceptability limits can be applied to higher-standard environment. Figure 17 might be not suitable for situations and that the outdoor air temperature is beyond the limits (5–33 °C). When the ambient temperature is beyond the limits, the thermal conditions in a naturally ventilated building may become intolerable.

With high ventilation rate in natural ventilation, the indoor air quality greatly depends on the ambient air quality, instead of affected by indoor pollutant source. However, if the ambient air is severely polluted, solely the natural ventilation will definitely increase the occupants' exposure to the high ambient pollutant level. Therefore, a hybrid ventilation design may be the only option [37].

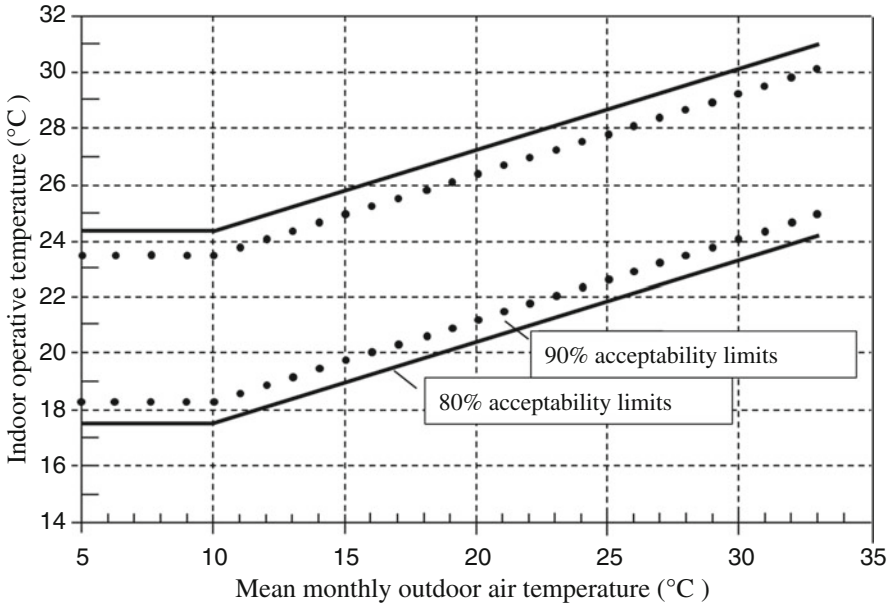


Fig. 17 Acceptable indoor operative temperature under natural ventilation conditions [38]

A general procedure for natural ventilation design includes architectural plan, system layout, component selection, opening size calculation, control strategy development, and detailed design drawing. Architects and engineers need to set the global geometric configuration considering dominant weather conditions and unusual conditions first. Then, the designer will design the airflow paths from the inlet to the outlet to achieve the desired airflow thermal comfort and ventilation rate and select the airflow components such as windows, doors, and solar chimneys to obtain desired control of airflow. Subsequently, the opening size will be calculated to meet the desired ventilation rate and indoor temperature. A controlling strategy for ventilation varying with the operating conditions must be developed. Finally, the detailed drawing about the system must be developed so that it can be built.

Vent Sizing

The opening size is calculated based on certain geometry, climate, building's configuration, and so on. Besides, the opening size is also related to the opening distribution, which is a part of the ventilation strategy. The methods for opening size calculation include direct methods and indirect methods, which will be introduced later. The general procedures for vent sizing is to design the main flow paths and size ventilation openings to satisfy the necessary ventilation rates in each zone of a building. When the configuration of openings and flow path in the building is

determined, the ventilation rate will be mostly determined by the natural driving forces. As a result, it is important to harness the dominant winds and enhance stack forces in the building at the design stage.

Direct Methods

Direct methods are derived from simple buildings where the ventilation rate is a simple function of the governing parameters [37]. Five of these methods are discussed by Allard [39].

For cross-ventilation in a building with two effective openings, the natural driven (wind-driven) force can be calculated as

$$\Delta P_w = \frac{1}{2} \rho C_{P1} v^2 - \frac{1}{2} \rho C_{P2} v^2 \quad (37)$$

The ventilation rate q is expressed as

$$q = C_d A^* \sqrt{\frac{2 \Delta P_w}{\rho}} \quad (38)$$

$$A^* = \left[\frac{1}{(A_t)^2} + \frac{1}{(A_b)^2} \right]^{-\frac{1}{2}} = \frac{A_t A_b}{\sqrt{A_b^2 + A_t^2}} \quad (39)$$

where A^* is the effective opening area, A_t is the area of the top opening, and A_b is the area of the bottom opening. A^* can be deduced as

$$A^* = \frac{\sqrt{\rho} q}{C_D \sqrt{2 \Delta P_w}} = 1.639 \frac{q}{v \sqrt{\Delta C_p}} \quad (40)$$

Then, the area of each individual opening can be obtained:

$$A_t = A_b = \sqrt{2} A^* \quad (41)$$

For stack ventilation in a building with two effective openings, the natural driven (buoyancy-driven) force can be calculated as

$$\Delta P_s = (\rho_o - \rho_i) g h \quad (42)$$

In addition, the effective opening area A^* , the top opening area A_t , and the bottom opening area A_b can also be deduced from the ventilation rate q . The derivation process is as follows:

$$q = C_d A^* \sqrt{\frac{2 \Delta P_s}{\rho_o}} = C_d A^* \sqrt{\frac{2 g h (T_i - T_o)}{T_o}} \quad (43)$$

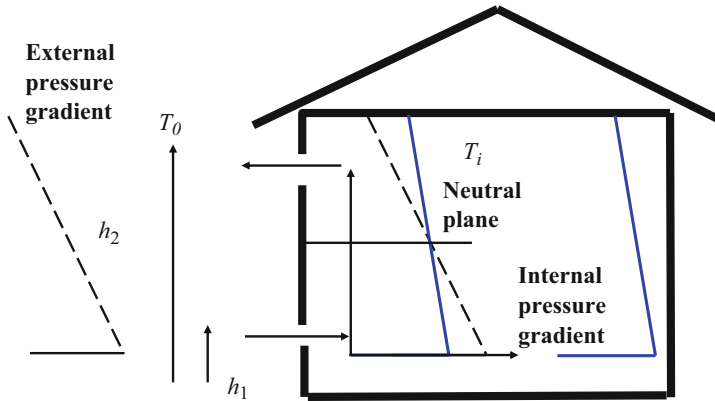


Fig. 18 Vent sizing for stack ventilation using the concept of neutral plane

$$A^* = \frac{\sqrt{T_o}q}{C_D\sqrt{2gh(T_i - T_o)}} \tag{44}$$

$$A_t = A_b = \sqrt{2}A^* \tag{45}$$

For a building with two effective openings combining wind and stack ventilation together, the natural driven (wind- and buoyancy-driven) force can be calculated as

$$\Delta P_s + \Delta P_w = (\rho_o - \rho_i)gh + \frac{1}{2}\rho C_{P1}v^2 - \frac{1}{2}\rho C_{P2}v^2 \tag{46}$$

The ventilation rate q and the effective opening area A^* can be expressed as

$$q = C_dA^*\sqrt{\frac{2gh(T_i - T_o)}{T_o} + 2\frac{\Delta P_w}{\rho}} \tag{47}$$

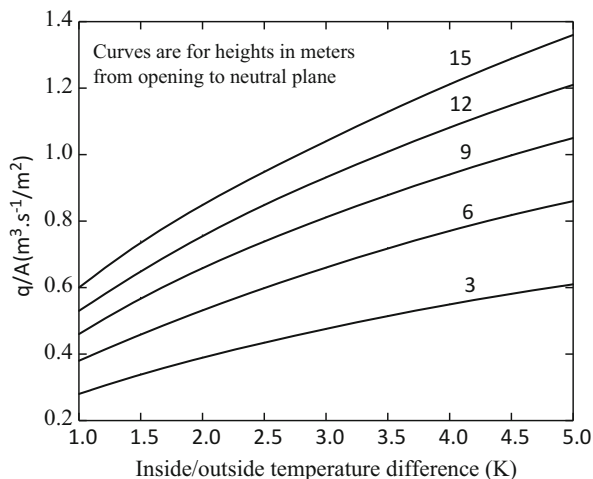
$$A^* = \frac{q}{C_D\sqrt{2gh\frac{T_i - T_o}{T_o} + 2\frac{\Delta P_w}{\rho}}} \tag{48}$$

If the neutral level h_n is a predefined parameter in a stack-ventilated building, the pressure difference and ventilation rate can be expressed using the concept of neutral plane according to Fig. 18 and Eqs. (46) and (47):

$$\Delta P_s = (\rho_o - \rho_i)g(h - h_n) = \rho_o g(h - h_n)\frac{T_i - T_o}{T_o} \tag{49}$$

$$q = C_dA^*\sqrt{2g(h - h_n)\frac{(T_i - T_o)}{T_o}} \tag{50}$$

Fig. 19 CIBSE design chart [40]



With the known parameters including neutral level h_n and the flow rate q , the effective area A^* , the top opening area A_t , and the bottom opening area A_b can be solved.

With the inside and outside temperature difference ($T_i - T_o$) and the height from opening to neutral plane ($h - h_n$), the airflow rate per unit area can be looked up from the CIBSE design chart [40] (as shown in Fig. 19). Then, the opening area can be deduced from the necessary ventilation rate.

Indirect Methods

Indirect methods try different opening size combinations and identify the best one based on network models. Among them, the LOOP pressure equation-based method presented by Axley [41] is the most commonly used one. The general LOOP method design procedure is to layout the global geometry, topology, and loops of the building first. Then, it identifies each pressure node. After determining the design conditions such as wind speed and direction, wind pressure coefficient, designed outdoor temperature, desired interior temperature, and other design requirements, the LOOP pressure equations can be formed, and the minimum feasible sizes can be determined. Subsequently, the remaining minimum feasible sizes are reevaluated in the same way, and an operational strategy can be devised. Figure 20 shows an example of a three-story ward building through using LOOP method. Six LOOP pressure equations can be formed for this building.

Natural Ventilation in Industrial Buildings

For industrial buildings, the ventilation rate needed is high as extra heat, humidity, and air pollutants (particles, harmful gases, etc.) may be generated during the industrial processes. The natural ventilation design for industrial buildings in this section refers to the national standard GB 50019–2003 in China [42].

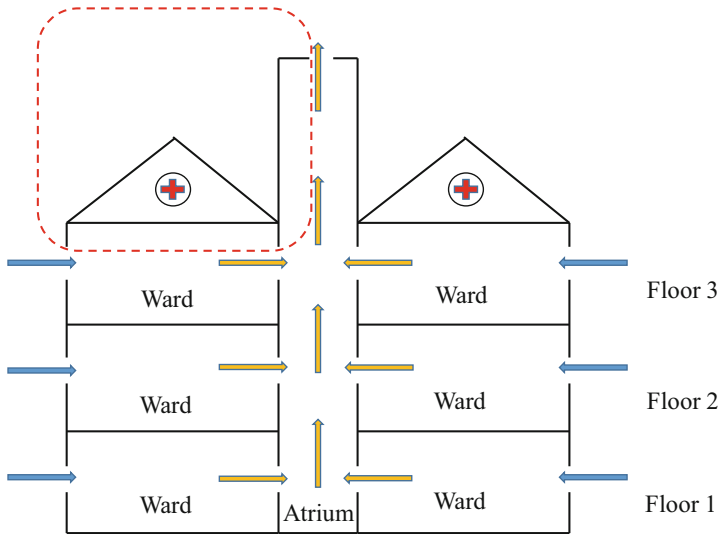


Fig. 20 LOOP pressure equation-based method

It is assumed that the natural ventilation rate is stable and the factors influencing the ventilation rate do not change with time. The design temperature inside the building is taken as the average temperature t_{ave} which can be calculated as

$$t_{ave} = \frac{t_i + t_e}{2} \tag{51}$$

where t_e is the exhaust temperature and t_i is the temperature at work area which is within 2 m above the ground. The location of the window, the design air supply rate, and the exhaust rate can be determined according to the dominant wind direction, heat source and pollutant source inside and around the building, etc. Then, the pressure differences between the inside and outside of the openings and the opening size can be calculated.

The ventilation rate q (kg/s) required to remove the excess heat from the work area can be obtained from Eq. (52):

$$q = \frac{Q}{c(t_e - t_s)} \tag{52}$$

where Q (kJ/s) is the total excess heat of the building, t_e (°C) is the air exhaust temperature at the upper part of the work area, t_s (°C) is the air supply temperature of the work area which can be valued as the outdoor design temperature in summer, c is the specific heat of air, and $c = 1.10$ kJ/(kg·°C). The exhaust temperature at the upper part of the work area can be determined based on the temperature gradient method and the effective heat coefficient method. The formed one is suitable for the

Table 6 The recommended design temperature at work area in summer (t_i) [42]

Outdoor design temperature for summer ventilation t_o (°C)	Design temperature at work area t_i (°C)
≤ 29	<32
30	<33
31	<34
32–33	<35
34	<36

Table 7 The temperature gradient (β) [42]

Building heat dissipation (W/m ³)	Building height (m)										
	5	6	7	8	9	10	11	12	13	14	15
12–43	1.0	0.9	0.8	0.7	0.6	0.5	0.4	0.4	0.4	0.3	0.2
24–47	1.0	1.2	0.9	0.8	0.7	0.6	0.5	0.5	0.5	0.4	0.4
48–70	1.5	1.5	1.2	1.1	0.9	0.8	0.8	0.8	0.8	0.8	0.5
71–93	–	1.5	1.5	1.3	1.2	1.2	1.2	1.2	1.1	1.0	0.9
94–116	–	–	–	1.5	1.5	1.5	1.5	1.5	1.5	1.4	1.3
							0.5	0.5			

Remark: The table is not suitable for buildings' height higher than 15 m

industrial buildings with uniform heat dissipation less than 116 W/m², and the latter one is suitable for industrial buildings with strong heat sources.

If the work area has uniform heat dissipation no more than 116 W/m², the indoor air temperature distribution along the height is roughly linear. Through the temperature gradient method, the exhaust temperature t_e of the upper part in the work area can be calculated:

$$t_e = t_i + \beta(h - 2) \quad (53)$$

where h (m) is the height between the center of the window and the ground; t_i (°C) is the design temperature at work area, which can be looked up through Table 6; and β (°C/m) is the temperature gradient along the height, which can be determined, as shown in Table 7.

For buildings with strong heat source, the distribution of air temperature along the height direction is complicated. Some of the thermojet generated from the heat source exhausts through the skylight and the other part is re-entrained to the work area through the turbulence of the airflow. The circulating airflow returning to the work area rises the temperature of air in the work area. Besides, the heat generated by the re-entrain air is called the effective excess heat. If the total excess heat produced from the heat source is Q , the effective excess heat that directly enters into the work area will be αQ . Here, α is defined as the effective heat coefficient.

According to the heat balance of the whole building, the required ventilation rate to remove the excess heat can be calculated as

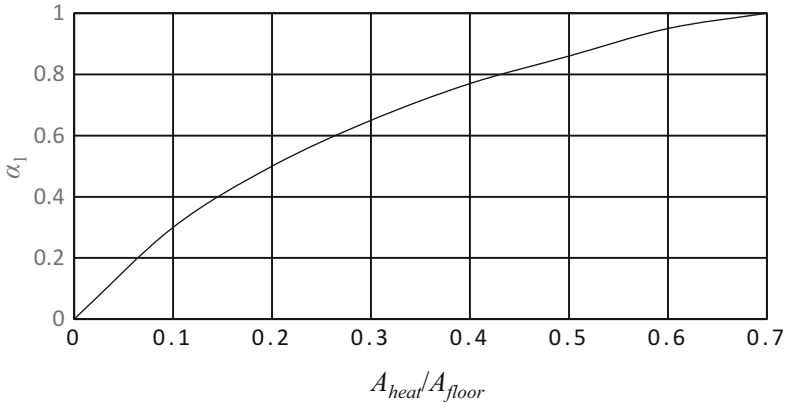


Fig. 21 The value of α_1 [42]

$$q = \frac{Q}{c(t_e - t_o)} \tag{54}$$

According to the heat balance of the work area, the required ventilation rate to remove the effective excess heat can be calculated as follows:

$$q' = \frac{\alpha Q}{c(t_i - t_o)} \tag{55}$$

As $q = q'$, Eqs. (54) and (55) can be changed into

$$\frac{Q}{c(t_e - t_o)} = \frac{\alpha Q}{c(t_i - t_o)} \quad \alpha = \frac{t_i - t_o}{t_e - t_o} \tag{56}$$

Therefore,

$$t_e = t_o + \frac{t_i - t_o}{\alpha} \tag{57}$$

According to Eq. (57), under the same t_e , the bigger the α , the more effective the excess heat enters into the work area and the higher the temperature at the work area. Consequently, t_e can be obtained by determining the value of α . The α value depends on the properties, distribution, and height of the heat source, which also depends on some geometric factors of buildings.

The effective heat coefficient can be determined by Eq. (58):

$$\alpha = \alpha_1 \alpha_2 \alpha_3 \tag{58}$$

where α_1 is the coefficient determined by ratio of heat source area (A_{heat}) to floor area (A_{floor}), α_2 is the coefficient determined by the height of heat source (h_{heat}), and α_3 is the coefficient determined by the ratio of the heat radiation (Q_f) to the total heat dissipation (Q) (Fig. 21).

Table 8 The value of α_2 [42]

Height of heat source (h_{heat})	≤ 2	4	6	8	10	12	≥ 14
α_2	1.0	0.85	0.75	0.65	0.60	0.55	0.5

Table 9 The value of α_3 [42]

Q_f/Q	≤ 0.4	0.5	0.55	0.6	0.65	0.7
α_3	1.0	1.07	1.12	1.18	1.30	1.45

The air supply opening area A_s and the air exhaust opening area A_e can be expressed as

$$A_s = \frac{q_s}{v_s \sqrt{2gh_s(\rho_o - \rho_i)\rho_o}} \quad (59)$$

and

$$A_e = \frac{q_e}{v_e \sqrt{2gh_e(\rho_o - \rho_i)\rho_o}} \quad (60)$$

where the subscripts s and e indicate the air supply opening and the air exhaust opening, respectively (Table 8).

Example for Natural Ventilation

If properly used, natural ventilation can enhance indoor air quality as well as satisfy occupants' thermal comfort without the consumption of energy (Table 9). However, the ventilation rate and airflow distribution are highly influenced by local meteorological conditions. In this section an existing example using natural ventilation in Guiyang City will be introduced and analyzed. Guiyang City is located $26^{\circ}35'$ north latitude and $106^{\circ}43'$ east longitude, the southwest of China, where the climate is hot in summer and cold in winter. The annual average temperature is 15.3°C in Guiyang City, and the outdoor design temperature is 30.1°C in air conditioning condition and 27.1°C in ventilation condition in summer. The average wind speed is 2.1 m/s , and the dominant wind direction is south. Besides, a school building in Guizhou University lying in Guiyang City is designed as a demonstration of green architecture which uses natural ventilation to save energy. Its architecture blueprint is shown in Fig. 22. The building is 24 m in height, including six floors with a basement floor. Atrium is used to enhance the buoyancy-driven ventilation, and electrical skylight is settled on the roof with vents facing the south and north. The skylight is in the middle of the roof so that the wind pressure coefficient on the roof is negative which can ensure the airflow exhaust from the roof. Besides, the roof of the skylight is inclined so that the area of northern vent is bigger than that of the southern vent. The vent size is 73.7 m^2 at the south and 114.7 m^2 at the north.



Fig. 22 A school building in Guizhou University

The airflow distribution of natural ventilation is complicated, which varies with the outdoor climatic conditions. All the outdoor temperature, wind speed, and wind direction can have a great influence on the airflow distribution. The airflow distribution is simulated using EnergyPlus in some typical conditions in summer, and the corresponding airflow distribution sketch maps are shown in Fig. 23. When the outdoor wind speed is very small, buoyancy is the mainly driven force for natural ventilation. The air flows into the building through openings at floor 1–4 and exhausts from the openings at top floor and skylight, which can be found in Fig. 23a. With the increment of the wind speed, the northern opening in floor 5 becomes inlet, and the southern opening in floor 4 becomes outlet when the outdoor wind direction is the north (see Fig. 23b). When the wind direction is the south, the openings at the south become inlets, and the openings at the north in the top two floors become outlets (see Fig. 23c). Figure 23a–f presents the comparison of the airflow distributions inside the building varying with the change of outdoor wind speed and direction. The fact that the vents on skylight keep as outlets is meaningful for the air quality inside the building.

The time length that meets the thermal comfort of 80% occupants (recommended by ASHARE Standard 55–2010 [38]) of this building on the design day is illustrated in Fig. 24. The letter “F” on the figure’s horizontal axis means “floor,” “S” means the opening of the room faces the south, and “N” indicates the opening of the room faces the north. Obviously, the comfort time brought from natural ventilation is long in Guizhou. The average climate temperature in summer is 23.2 °C or so, making natural ventilation possible to lower the indoor temperature. At noon and afternoon, the solar radiation and heat transfer through building envelopes make the indoor temperature high. Whether natural ventilation can satisfy the thermal comfort

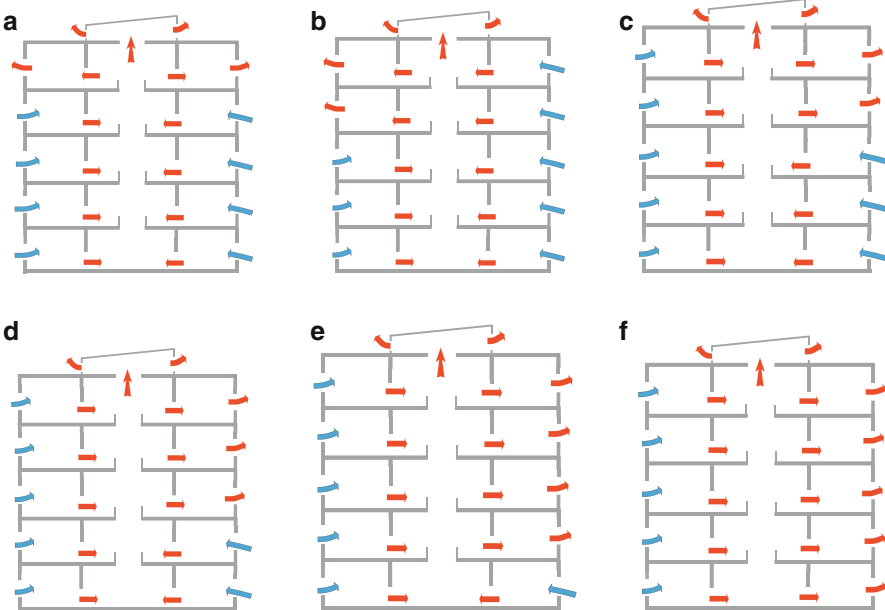


Fig. 23 Sketch maps of airflow distribution. (a) Wind speed: 0.25 m/s. Wind direction: N. (b) Wind speed: 1.30 m/s. Wind direction: N. (c) Wind speed: 2 m/s. Wind direction: S. (d) Wind speed: 2.65 m/s. Wind direction: S. (e) Wind speed: 4 m/s. Wind direction: N. (f) Wind speed: 4.93 m/s. Wind direction: N

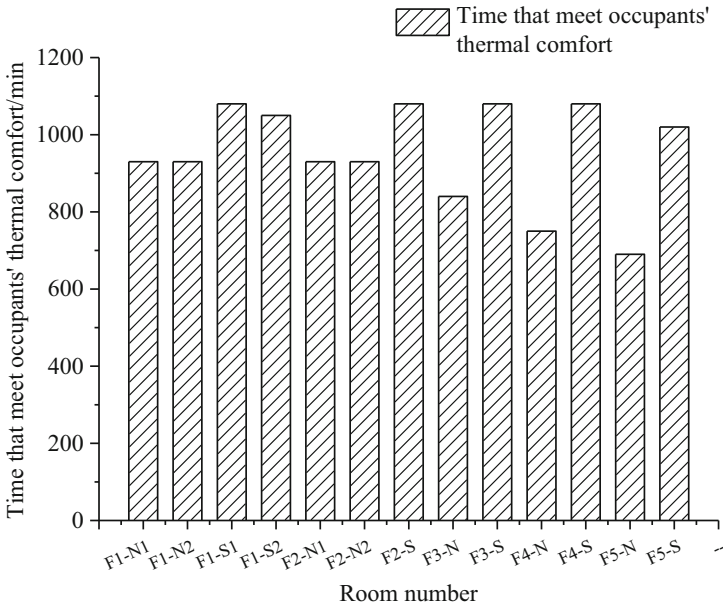


Fig. 24 The time period that meet occupants' thermal comfort on design day

depends on the ventilation rate and the temperature difference inside and outside. It is obvious that the thermal comfortable time is longer in southern rooms than in northern rooms. The proportion of thermal comfortable time is 75% in the room with south-facing window, while that is 52% in the room with north-facing window on floor 4 at the design day, which is due to that the dominant wind direction is the south and the ventilation rate is higher in rooms with south-facing windows to remove heat. Because the airflow direction is from the bottom to top and the cool outdoor air flows into lower floors first, the thermal comfortable time length in upper floors is shorter than that in lower floors.

The cooling load reduced by natural ventilation is related to the ventilation rate and the outdoor temperature. Natural ventilation cannot always act as a cooling method when the outdoor temperature is high and the indoor temperature is low due to the thermal storage effect of the building envelopes. In general, the cooling load reduced by natural ventilation is large at night as the outdoor temperature is low and is relatively small at noon and afternoon as the outdoor temperature is relatively high. The results of the school building in Guizhou University present that natural ventilation can reduce the cooling load by 10^4 – 10^5 W, which can highly reduce the energy consumption of air conditionings.

Natural ventilation is highly dependent on local climate. According to the above analysis, natural ventilation can satisfy the thermal comfort in most cases in Guiyang City where the average air temperature in summer is relatively low. For regions with bad weather conditions, the combination of natural ventilation and air conditioning systems could be considered.

Conclusion and Future Directions

Natural ventilation is the flow of outdoor air caused by wind and thermal pressures through intentional openings into the building's shell. Generally, natural ventilation can provide a high ventilation rate more economically than mechanical ventilation, yet its airflow and temperature are significantly dependent on the outdoor climate. Therefore, it is difficult to analyze and predict natural ventilation.

There are two types of natural ventilation occurring in buildings, respectively, wind-driven ventilation and buoyancy-driven ventilation; among which, wind-driven ventilation arises from different pressures created by wind around a building or structure. The wind pressure coefficients are important parameters for flow rate calculation. Some empirical values and deductive methods can be used for the prediction of simple buildings. Buoyancy-driven ventilation is driven by the directional buoyancy force, resulting from temperature differences between the interior and exterior. The concept of neutral plane is important for the airflow direction of buoyancy-driven ventilation. The predict models of natural ventilation include single-zone model, multi-zone model, and CFD model. The single-zone model is easy to understand and utilize, which can be used to analyze and design simple buildings. An example of multi-zone model, the MIX model, is based on the calculation of pressure differences between different zones. The ventilation rate through each opening can be solved by pressure difference between two sides of

opening, which is driven by wind or buoyancy. The CFD model is the application of computational fluid dynamics in building ventilation, which uses numerical methods to solve the partial differential equations of momentum, energy, and mass. Air temperature, pressure, airflow rate, water vapor pressure, pollutant concentration, and turbulence coefficient can all be obtained through solving the CFD model. However, for large buildings, the solving process is time-consuming, and the boundary conditions are difficult to control.

To measure the natural ventilation rate, tracer gas methods are the most reliable and commonly used ways. Three existing methods including the concentration decay method, the constant injection method, and the constant concentration method are appropriate ways for the determination of air change rate. Concentration decay method is the process of releasing a small amount of tracer gas into the room at first and recording the indoor tracer gas concentration with regular time intervals after the tracer gas is well-mixed. Since it is easy to operate, concentration decay method is the most commonly used one in practice. Moreover, the needed amount of tracer gas for concentration decay method is much less than the constant injection method. However, it cannot reflect the timely fluctuation of ventilation rate as it assumes that the ventilation rate is constant during the measurement. Constant injection method is the process that a certain amount of tracer gas is released constantly during the measurement. The indoor tracer gas concentration increases with time, which finally reaches the equilibrium concentration. As it takes a long time to reach the equilibrium concentration, constant injection method is time-consuming and tracer-gas-consuming, and it cannot measure the timely fluctuation of ventilation rate either. Constant concentration method is the process of keeping the indoor tracer gas concentration a predefined value, which monitors and controls the indoor tracer gas concentration through using an automated dosing and control system. This method has an advantage of detecting the ventilation rate timely, and even short-term changes of ventilation rate can be measured. Nevertheless, the high-cost equipment and operation make this method be rarely used for indoor air quality evaluation. Commonly, N_2O , SF_6 , and CO_2 are the most frequently used tracer gases.

The general natural ventilation form includes wind-driven form (e.g., cross-ventilation), buoyancy-driven form (e.g., single-side ventilation, chimney), and the combination of both wind- and buoyancy-driven forms. In natural ventilation technologies, atrium and solar chimney are often applied to improve the buoyancy-driven ventilation performance. Besides, the ventilation cap is a useful accessory to improve the wind-driven ventilation performance. Wind-proofed shields are often used in the skylight to prevent air from flowing into the building through skylights.

There are three elements for the design of ventilation. Firstly, the ventilation rate must be large enough to meet the current standards or guidelines. Secondly, air should flow from clean areas to unclean areas. Thirdly, the indoor airflow distribution should be uniform and avoided from blind corners. After determining the geometric configuration of the building, the designed temperature, and the airflow rate, the opening size can finally be calculated. Methods for vent sizing include direct methods and indirect methods. Direct methods are derived from simple buildings where the ventilation rate is a simple function of the governing parameters. Besides,

direct methods include simple function calculation and chart-lookup method. Indirect methods try different opening size combinations and identify the best one using network models. Among the indirect methods, the LOOP pressure equation-based method presented is the most commonly used one, and some exiting examples also reveal the great potential of natural ventilation.

Acknowledgements The study has been supported by The National Natural Science Foundation of China (Grant No. 51378103) and The National Key Research and Development Program of China (Grant No. 2016YFC0700500).

References

1. Wang JN, Cao SR, Li Z et al (1998) Human exposure to carbon monoxide and inhalable particulate in Beijing, China. *Biomed Environ Sci Bes J* 1(1):5–12
2. Fanger PO, Lauridsen J, Bluysen P et al (1988) Air pollution sources in offices and assembly halls, quantified by the olf unit. *Energy Buildings J* 12(1):7–19
3. ASHARE (2017) ASHRAE handbook: fundamentals. Atlanta, GA: American Society of Heating, Refrigerating, and Air-Conditioning Engineers, Inc.
4. Xu Y (2004) Fengshui in China: geomantic divination between state orthodoxy and popular religion (review). *China Rev Int J* 11(1):35–41
5. Laussmann D, Helm D (2011) Air change measurements using tracer gases: methods and results. Significance of air change for indoor air quality. In: Mazzeo N (ed) *Chemistry, emission control, radioactive pollution and indoor air quality*. ISBN:978-953-307-316-3
6. Fan CY, Lin ZP (2002) Current situation and development of residential environment equipment. *HVAC J* 32(4):34–42
7. Li YG, Angelo D, Jeff S (2000) Prediction of natural ventilation in building with large openings. *Building Environ J* 35(3):191–206
8. Pérez-Lombard L, Ortiz J, Pout C (2008) A review on buildings energy consumption information. *Energy Buildings J* 40(3):394–398
9. Harvey DLD (2013) Recent advances in sustainable buildings: review of the energy and cost performance of the state-of-the-art best practices from around the world. *Ann Rev Environ Resour J* (38):281–309
10. ASHRAE (2004) Air leakage performance for detached single-family residential buildings. ANSI/ASHRAE Standard 119–1988(RA 2004)
11. NRCC (1995) National building code of Canada. National Research Council of Canada, Ottawa
12. Qian H, Li YG, Seto WH et al (2010) Natural ventilation for reducing airborne infection in hospitals. *Building Environ J* 45(3):559–565
13. CDC (2003) Guidelines for environmental infection control in health-care facilities. U.S. Department of health and human services center for disease control and prevention (CDC), Atlanta
14. Hubad B, Lapanje A (2012) Inadequate hospital ventilation system increases the risk of nosocomial mycobacterium tuberculosis. *J Hosp Infect J* 80(1):88–91
15. Li YG, Keung M, Seto WH, Yuen PL, Leung J, Kwan JK, Yu SCT (2008) Factors affecting ventilation effectiveness in SARS wards. *Hong Kong Med J J* 14(Suppl 1):33–36
16. Li YG, Ching WH, Qian H, Yuen PL, Seto WH, Kwan JK, Leung JKC, Leung M, Yu SCT (2007) An evaluation of the ventilation performance of new SARS isolation wards in nine hospitals in Hong Kong. *Indoor Built Environ J* 16(5):400–410
17. Fraser VJ, Johnson K, Primack J et al (1993) Evaluation of rooms with negative pressure ventilation used for respiratory isolation in seven midwestern hospitals. *Infect Control Hosp Epidemiol Off J Soc Hosp Epidemiol Am J* 14(11):623–628

18. Pavelchak N, Cummings K, Stricof R et al (2001) Negative-pressure monitoring of tuberculosis isolation rooms within New York state hospitals. *Infect Control Hosp Epidemiol J* 22(8):518–519
19. Riley EC, Murphy G, Riley RL (1978) Airborne spread of measles in a suburban elementary school. *Am J Epidemiol J* 107(5):421–432
20. Waxham FE (2002) The outdoor treatment of tuberculosis. *J* 21:2754
21. Qian H (2007) Ventilation for controlling airborne infection in hospital environments. PhD thesis, The University of Hong Kong
22. WHO (1999) Guidelines for the prevention of tuberculosis in healthcare facilities in resource-limiting settings. World Health Organ, Geneva
23. Cox H, Escombe R, Mcdermid C et al (2012) Wind-driven roof turbines: a novel way to improve ventilation for TB infection control in health facilities. *PLoS One* 7(1):e29589. <https://doi.org/10.1371/journal.pone.0029589>
24. Escombe AR, Oeser CC, Gilman RH et al (2007) Natural ventilation for the prevention of airborne contagion. *Plos Med J* 4(2):e68. <https://doi.org/10.1371/journal.pmed.0040068>
25. Apisarnthanarak A, Mundy LM (2006) Influenza outbreak among health care workers in an avian influenza (H5N1)-endemic setting. *Clin Infect Dis J* 43(11):1493–1494
26. Heiselberg P, Centre HV (2000) Principles of hybrid ventilation. Hybrid ventilation Centre Aalborg University, Aalborg
27. Linden PF (1998) The fluid mechanics of natural ventilation. *Ann Rev Fluid Mech J* 31(31):309–335
28. Awbi HB (1991) Ventilation of buildings[M]. E & FN Spon, London
29. Liddament MW (1986) Air infiltration calculation techniques – an application guide, International network for information on ventilation. Air infiltration and Ventilation Center, Brussels
30. Miguel AF, Silva AM (2000) Porous materials to control climate behavior of enclosures: an application to the study of screened greenhouses. *Energy Building J* 31:195–209
31. Miguel AF, Braak NJVD, Bot GPA (1997) Analysis of the airflow characteristics of greenhouse screening materials. *J Eng Res J* 67(2):105–112
32. Valera DL, Molina FD, Alvarez AJ et al (2005) Contribution to characterisation of insect-proof screens: experimental measurements in wind tunnel and CFD simulation. *Acta Horti J* 691:441–448
33. Bailey BJ, Montero JI, Perez PJ et al (2003) Airflow resistance of greenhouse ventilators with and without insect screens. *Biosyst Eng J* 86(2):217–229
34. Sherman MH (1990) Tracer-gas techniques for measuring ventilation in a single zone. *Building Environ J* 25(4):365–374
35. ASTM International (2001) ASTM standard E 741–00. Standard test method for determining air change in a single zone by means of a tracer gas dilution. American society for testing and materials
36. Mundt E, Mathisen HM, Nielsen PV et al (2003) Ventilation effectiveness. Rehva, Brussels
37. WHO (2009) Natural ventilation for infection control in health care settings. WHO Press, World Health Organization, Geneva
38. ASHRAE (2010) ASHARE Standard 55–2010. Thermal environmental conditions for human occupancy
39. Allard F (ed) (1998) Natural ventilation in buildings – a design handbook. Earthscan Publications Ltd, London
40. Engineers (2006) CIBSE Guide A. In: Air infiltration and natural ventilation, 4th edn. Chartered Institution of Building Services Engineering, London
41. Axley J (1998) Introduction to the design of natural ventilation systems using loop equations. In: Proceedings of the 19th AIVC conference on ventilation technologies in urban areas, Oslo, 28–30 Sept 1998, pp 47–56
42. Ministry of Construction, PR China, AQSIQ (State Administration for Quality Supervision and Inspection and Quarantine, PR China) (2015) GB 50019–2015, Code for design of heating ventilation and air conditioning [S]